BRNO UNIVERSITY OF TECHNOLOGY

ESCUELA POLITÉCNICA DE INGENIERÍA DE GIJÓN

MASTER IN INDUSTRIAL ENGINEERING

FACULTY OF CIVIL ENGINEERING

STRESS STATE OF SPECIMEN WITH INITIAL CHEVRON NOTCH

D. GONZÁLEZ MENÉNDEZ SOFÍA

SUPERVISOR: SOBEK JAKUB

SUPERVISOR SPECIALIST: SEITL STANISLAV

DATE: MAY 2017

Abstract

The thesis is focused on the problematic of the numerical modelling of the so-called chevron-notched fracture test specimens – specimens with the initial stress concentrator in the form of the V-shape notch. This research project consists of the use of the FE software ANSYS to develop a 2D numerical model automatically (by the proper macro file with different input parameters) and describe the stress state around the crack tip by linear elastic fracture mechanics approach generalized into value of the stress intensity factor *K* (which is being changed according to the different values of the input parameters).

Keywords

Linear elastic fracture mechanics, numerical modelling, FEM, chevron-notched specimen, stress intensity factor, 3PB test, 4PB test.

This thesis constitutes the conclusion to my Master in Industrial Engineering with specialization in construction (2015—2017) of the University of Oviedo. This Project is realized during an Erasmus mobility in Brno University of Technology in the Faculty of Civil Engineering.

From here I would like to express my thanks to my supervisors Stanislav Seitl, Jakub Sobek and María Jesús Lamela Rey for their support and supervision during the implementation of this project.

This thesis has been worked out under the project of the Czech Science Foundation (project No. 15-07210S) and project No. LO1408 "AdMaS UP – Advanced Materials, Structures and Technologies", supported by Ministry of Education, Youth and Sports under the „National Sustainability Programme I".

1. General Index

2. Figure Index

3. Resumen Español

BRNO UNIVERSITY OF TECHNOLOGY

ESCUELA POLITÉCNICA DE INGENIERÍA DE GIJÓN

MÁSTER EN INGENIERÍA INDUSTRIAL
FACULTAD DE INGENIERÍA CIVIL

ESTADO TENSIONAL DE UN ESPECIMEN CON MUESCA TIPO CHEVRON

D. GONZÁLEZ MENÉNDEZ SOFÍA

SUPERVISOR: SOBEK JAKUB

SUPERVISOR ESPECIALISTA: SEITL STANISLAV

FECHA: MAYO 2017

3.1 INTRODUCCIÓN

Nuestro entendimiento de como los materiales pueden fallar y nuestro conocimiento sobre cómo prevenir los fallos en las estructuras ha aumentado mucho en los últimos años.

Hay dos circunstancias básicas en las cuales pueden ocurrir los fallos en una estructura. La primera es durante la fase de diseño, construcción o durante el funcionamiento de la estructura. Esto puede ser debido a fallo humano (ignorancia, análisis inapropiado o falta d experiencia). El segundo tipo de fallo es el debido a la utilización de nuevos materiales, estos puedes comportarse de manera diferente a la esperada.

El campo de la mecánica de la fractura ha permitido prevenir un gran número de fallos durante los últimos años. Cuando se aplican correctamente los criterios de esta teoría, no sólo ayuda a prevenir los fallos en la etapa de diseño, sino que también ayuda a reducir la frecuencia de aparición de los mismos (Anderson, 2005).

Cómo se anuncia en el título de este trabajo, el tema que principal del que se va a tratar son los especímenes con muesca tipo chevron. La razón por la cual se ha decidido utilizar este tipo de especímenes es debido a todas las ventajas que se explican a lo largo del documento.

Este proyecto constituye el broche final a mi Máster en Ingeniería Industrial con especialización en construcción (2015-2017) en la Universidad de Oviedo. El proyecto fue realizado durante una movilidad Erasmus en la Universidad de Brno en la Facultad de Ingeniería Civil. Se trata de un proyecto de investigación que consiste en la utilización del software de elementos finitos ANSYS para hacer un análisis numérico y describir el estado de tensiones en las proximidades de la grieta utilizando especímenes con muesca tipo chevron.

Desde aquí me gustaría dar las gracias a mis tutores y asesores Staislav Seitl, Jakub Sobek y María Jesús Lamela Rey por su apoyo y supervisión durante la implementación de este proyecto.

3.2 ESTADO DEL ARTE

El hecho de evitar la fractura durante el diseño de las estructuras no es una idea nueva. Se puede observar en claros ejemplos como las antiguas pirámides de Egipto o incluso en las construcciones del Imperio romano. Se hace una breve descripción histórica de la utilización de los especímenes con muesca tipo chevron. En la segunda parte de ese mismo apartado se hace una descripción de porqué se ha decidido hacer el análisis sobre este tipo de especímenes y no con otro tipo de muesca, comentando brevemente algunas de las ventajas o inconvenientes de los mismos.

3.3 DESCRIPCIÓN DE LA FINALIDAD DEL PROYECTO

En este documento se va a explicar el análisis numérico realizado con el software ANSYS para estudiar el comportamiento de especímenes con muesca tipo chevron. Para conseguir esto el primer paso fue la búsqueda de información sobre el tema tanto en artículos científicos como en libros, páginas web y la biblioteca de la Universidad.

Durante el proyecto nos hemos centrado en la creación de un modelo 2D al cual se le han ido cambiando los distintos parámetros de entrada (por ejemplo, el número de capas, la geometría o las condiciones de contorno). Este modelo se creó de tal manera que al cambiar los parámetros de entrada se regenerara de manera automática con su propio archivo macro. También se realizó un estudio de cómo cambia el valor del factor de intensidad de tensiones en función de los distintos parámetros de entrada.

3.4 ANTECEDENTES TEÓRICOS

Se comentan brevemente todos los apartados teóricos que se consideran de interés para el lector del documento. En primer lugar, se habla de los distintos modos de carga básicos a los cuáles puede estar sometido el espécimen en cuestión. El documento y el proyecto se centran en el modo de carga I.

La mecánica de la fractura es un campo que se centra en el estudio de la propagación de las grietas en los distintos materiales. Se utilizan métodos analíticos para el cálculo de la fuerza en n la grieta y después mediante experimentos se puede caracterizar la resistencia a la fractura del material. Posteriormente se definen los distintos tipos de fractura que existen según la deformación producida.

- Frágil: se caracteriza por la separación del material en un plano perpendicular a la dirección en la cual se ha aplicado la carga. Este tipo de materiales presentan comportamiento elástico prácticamente hasta el pico de carga, punto en el cual la grieta se propaga a lo largo del espécimen.

- Quasi-frágil: Para este tipo de materiales, como puede ser el hormigón o algunas cerámicas, el comportamiento no lineal comienza antes de llegar al punto de carga máxima (es en ese punto donde la grieta empieza a propagarse).

- Dúctil: Este tipo de materiales presentan una importante deformación plástica previa. El comportamiento no lineal empieza mucho antes de que la grieta comience a propagarse.

La mayor parte de los materiales poseen pequeñas grietas, o contaminantes (por ejemplo, partículas ajenas) que hacen de concentrador de tensiones. Este es uno de los motivos por los cuales la tenacidad a la fractura real de un material es más pequeña que el valor teórico.

La serie de expansión e Williams trata de estimar los resultados de la parte no lineal. Esta zona juega un papel importantísimo en el fallo de los materiales frágiles.

El factor de intensidad de tensiones es una constante que caracteriza completamente las condiciones del entorno de la grieta en un material elástico lineal. Si conocemos el valor de esta constante, se puede conocer entonces el comportamiento de las tensiones en todo el entorno de la grieta. Se debe tener en cuenta que el factor de intensidad de tensiones es distinto del término concentrador de tensiones. El facto de intensidad de tensiones permite caracterizar el estado tensional en el frente de la grieta. La ruptura del material ocurrirá cuando este factor alcance un valor, característico de cada material, denominado tenacidad a la fractura.

3.5 MODELO

Tal y como se ha comentado previamente, el análisis numérico se realiza mediante la utilización del software de elementos finitos ANSYS. Se trata de un programa de simulación que ayuda a resolver algunos ejemplos de diseño bastante complejos.

Para la realización de este análisis solo se ha implementado la mitad del espécimen, ya que se trataba de una geometría simétrica. La utilización de la condición de tensión plana se basa en la posibilidad de simular la no uniformidad de las distintas capas utilizadas durante la simulación.

Para poder empezar con el desarrollo del modelo, el primer paso es tener muy clara la geometría que se va a modelar para poder introducirla correctamente en el programa. En este caso se han implementado 2 geometrías que se pueden apreciar en las siguientes figuras.

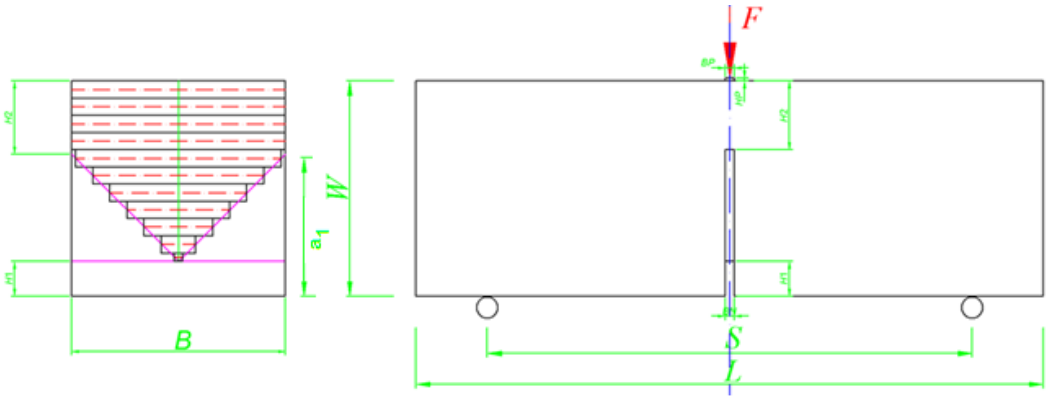

Figura 1. Esquema geometría 3PB utilizada

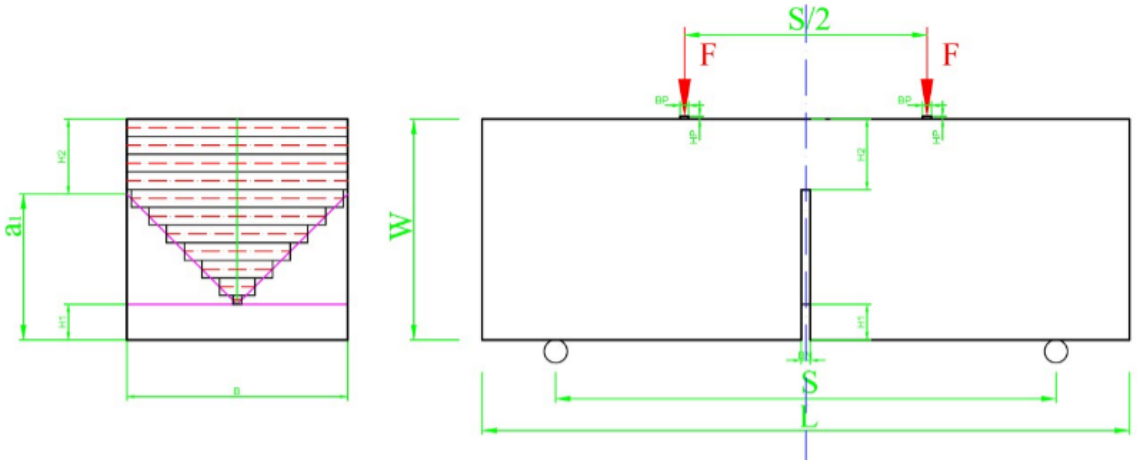

Figura 2. Esquema geometría 4PB utilizada

La primera figura se corresponde con la geometría 3PB utilizada para el primer análisis (Influencia del número de capas utilizado). Los parámetros utilizados para esta geometría fueron:

W = 0.1 m; B = 0.1 m; L = 0.4 m; S = 0.36 m; B_N = 0.003 m; N (variable)

La segunda imagen se corresponde con la geometría 4PB, utilizada para los otros dos análisis. Los parámetros empleados en este caso fueron:

W = 0.1 m; B = 0.1 m; L = 0.825 m; S = 0.8 m; B_N (variable); N = 30

Una vez que se tiene claro el modelo, Podemos pasar a su introducción en ANSYS. El código introducido en el programa se estructura en diferentes partes. Para ver exactamente el código ir al anexo de este mismo documento.

En primer lugar, se definen los parámetros que se van a utilizar. En este caso se creó un modelo de tal manera que se pudieran cambiar algunos de los parámetros de entrada, es por esto que la creación de bucles fue necesaria. El siguiente paso es la definición de los elementos y del material (las características específicas se explican más delante). En este caso se trataba de un modelo plano 2D por lo que el comando PLANE82 fue utilizado. Una vez que se ha definido el tipo de elemento, pasamos a la introducción de los nodos. En este caso se ha utilizado el comando KSCON para poder tener en cuenta la singularidad de la tensión en el inicio de la grieta.

Con todo esto definido correctamente podemos pasar a mallar el modelo. En nuestro caso se han definido dos mallas distintas, una para el caso del hormigón y otra para el acero utilizado en las plaquitas. El último paso antes de la resolución para obtener los resultados es la definición de las condiciones de contorno. Para este caso se han utilizado las condiciones de contorno más habituales en 3PB y 4PB, es decir, las componentes verticales y horizontales de la carga aplicada y nodos fijos en ambas direcciones en los soportes.

El último paso es el cálculo para la obtención de los resultados. Para esto se ha creado el modelo de tal manera que los parámetros son generados por el propio modelo. Se ha creado un documento de texto en el cual se van tabulando los resultados obtenidos con el programa.

A continuación, se explican con detalle los valores de las propiedades de los materiales introducidos en el programa.

Porpiedades de los materiales para 3PB

El espécimen utilizado estaba hecho de un material quassi-frágil, en este caso hormigón con módulo de elasticidad E = 35 GPa y coeficiente de poisson v = 0.2. las plaquitas utilizadas para aplicar la fuerza se fabricaron con acero con los siguientes valores de módulo de elasticidad E = 210 GPa y coeficiente de poisson v = 0.3. El valor de la fuerza aplicada para este estudio fue de 1000 N.

Propiedades de los materiales para 4PB

El espécimen en este caso se realizó con un material dúctil, en concreto aluminio con módulo de elasticidad E = 72.3948 GPa y coeficiente de poisson v = 0.3. Las plaquitas al igual que para el 3PB se fabricaron de acero con módulo de elasticidad E = 210 GPa y coeficiente de poisson v = 0.3. En este caso el valor de la fuerza aplicada fue de 100 N.

3.6 RESULTADOS Y DISCUSIÓN

Influencia del número de capas utilizadas

Para la obtención de los valores del factor de intensidad de tensiones se ha utilizado el comando KCALC. Los cálculos se realizaron cambiando los valores de los parámetros de tal manera que se pudo posteriormente estudiar los resultados obtenidos.

Para la realización del estudio se fue variando el número de capas de tal manera que N = 3, 5,7,9 y 10. También durante la realización de este estudio se tuvo en cuenta que el parámetro H_1 (longitud inicial de la grieta) es dependiente del valor relativo máximo de la longitud de la grieta H_2.

En la siguiente figura, se puede apreciar como el valor del factor de intensidad de tensiones depende de la longitud inicial de la grieta para un valor fijo de H_2 (para este primer caso se toma el valor de este parámetro igual a 0.5, esto significa la mitad del espécimen). Además, en esta figura se pueden apreciar dos cosas importantes:

- Los valores del factor de intensidad de tensiones se estabilizan a partir de un número de capas de 7 o más. Entre 9 y 10 capas las diferencias son prácticamente inapreciables.
- Con la división de la sección transversal en 3 capas, existe un estudio de estabilidad para el valor del factor de intensidad de tensiones donde se puede ver que para N=10 el

último valor es tres veces más grande. Una desviación similar se puede observar para N= 5.

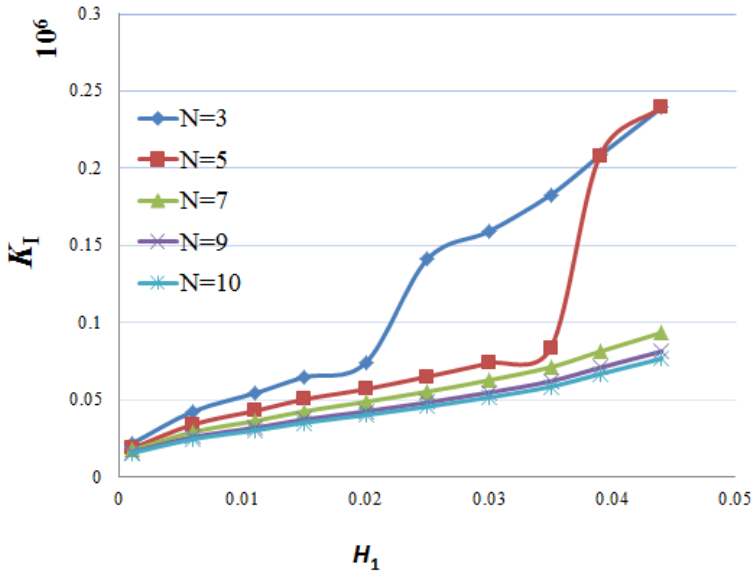

Figura 3. Resultados del Factor de Intensidad de tensiones correspondientes al distinto número de capas para H_2 =0.5

Un segundo análisis se realizó para los mismos valores del parámetro N, pero en este caso el valor de H2 utilizado fue 0.8 (esto implica que la parte sólida se corresponde con un 80% del ancho del espécimen). En la siguiente figura se puede ver que la tendencia es muy similar a la del caso anterior, de nuevo el número mínimo de capas para el cual se estabilizan los valores del factor de intensidad de tensiones es N = 7. Igual que en el caso anterior el número óptimo de capas es N = 10.

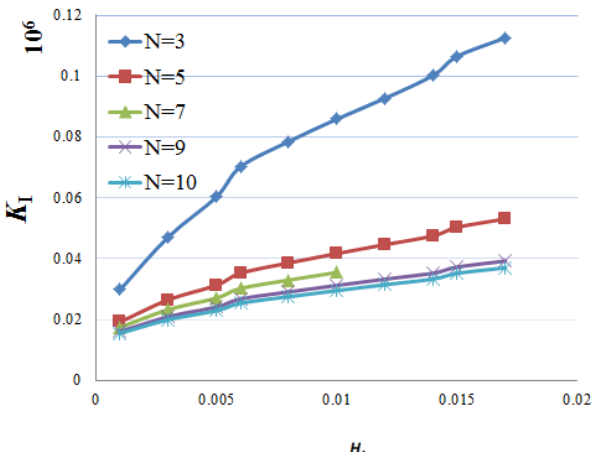

Figura 4. Resultados del Factor de Intensidad de tensiones correspondientes al distinto número de capas para H_2 =0.8

Influencia del ángulo

El Segundo análisis realizado se basó en el estudio de la influencia del ángulo. Para caracterizar el valor de dicho ángulo se utilizó en parámetro α_0 (valor inicial de la grieta, pero en este caso en valor relativo). Los cambios realizados en el valor de dicho parámetro se hicieron para comprobar la influencia que estos cambios tenían en el valor del factor de intensidad de tensiones. Para cada uno de los valores de α_0 se realizó un gráfico y posteriormente se realizó uno conjunto para poder comparar los distintos resultados obtenidos.

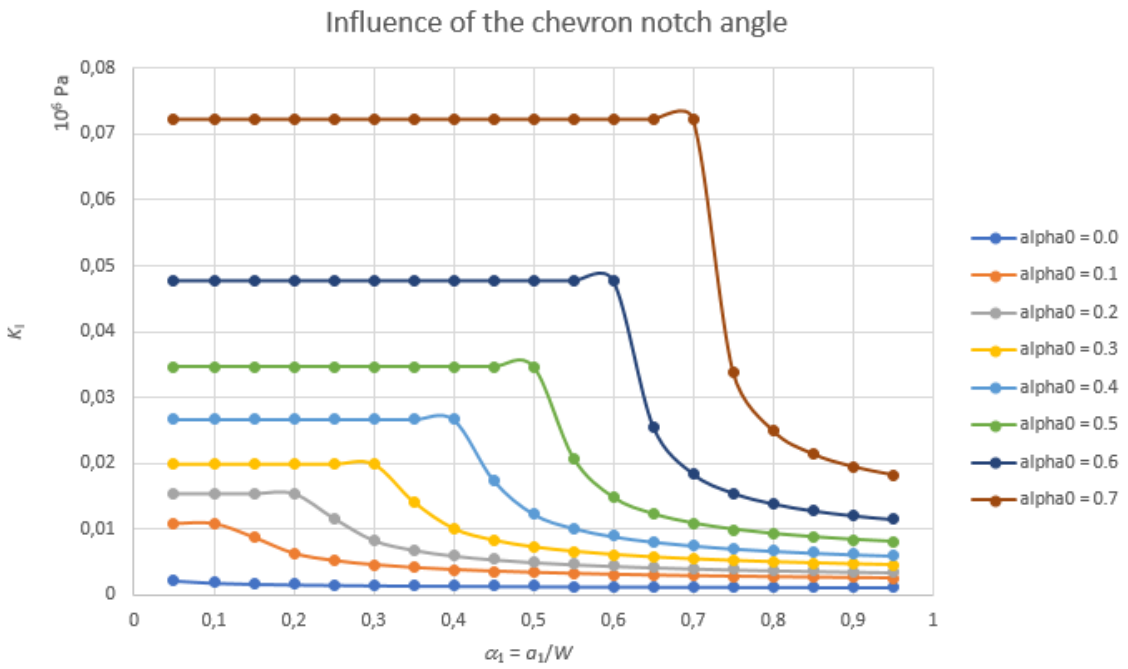

Figura 5. Gráfico comparativo de los resultados obtenidos para los diferentes valores de α_0

Influencia del espesor

Para el tercer y último análisis, el parámetro que se va a cambiar para ver el efecto que tiene sobre el valor del factor de intensidad de tensiones, es el espesor de la muesca chevron. Este análisis a su vez está dividido en dos sub-análisis que se explican a continuación.

El primer sub-análisis se trata de que para diferentes valores de α_0 (constantes para cada caso), se estudia que es lo que pasa con el valor del factor de intensidad de tensiones para diferentes valores de α_1 dependiendo del espesor.

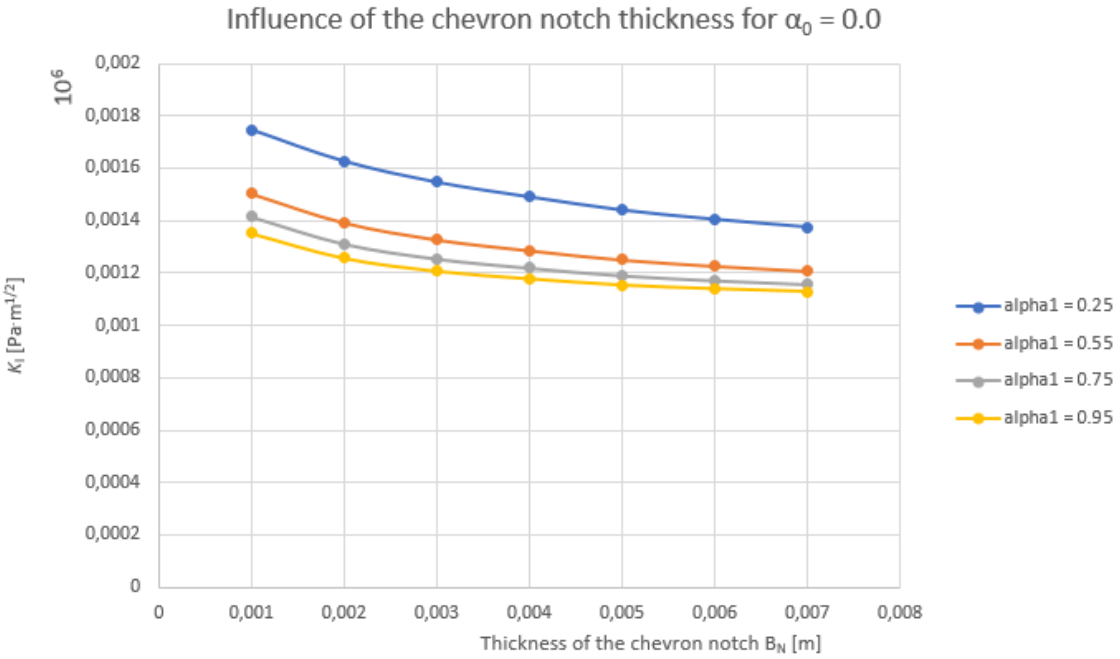

Figura 6. Influencia del espesor de la muesca chevron para diferentes valores de α_1 y α_0 = 0.0

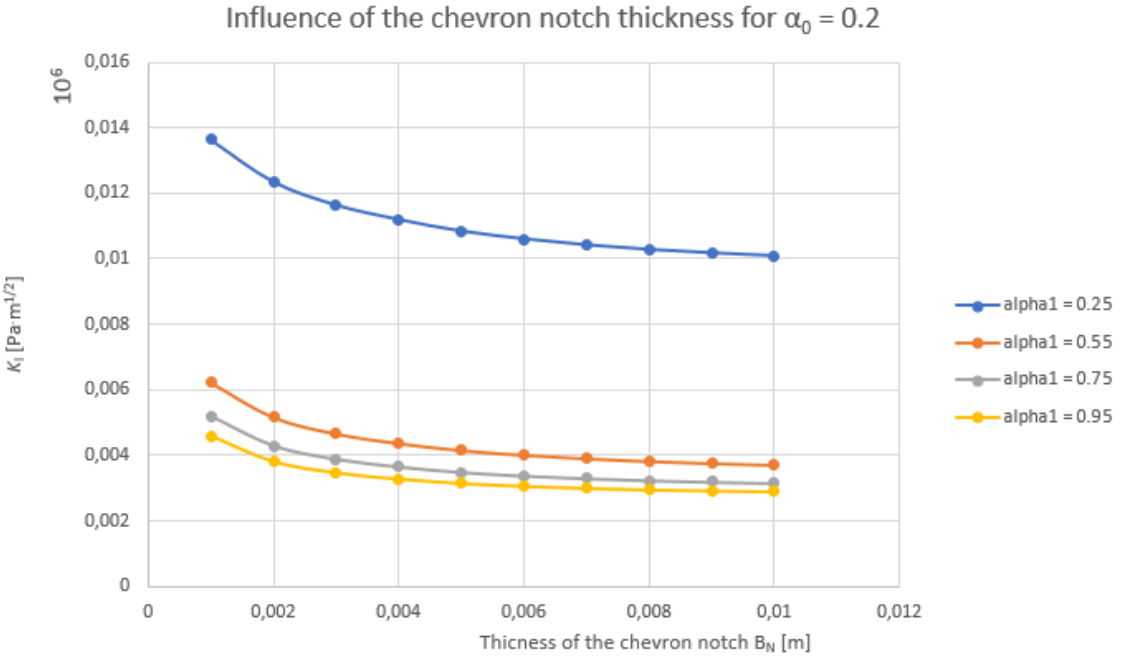

Figura 7. Influencia del espesor de la muesca chevron para diferentes valores de α_1 y α_0 = 0.2

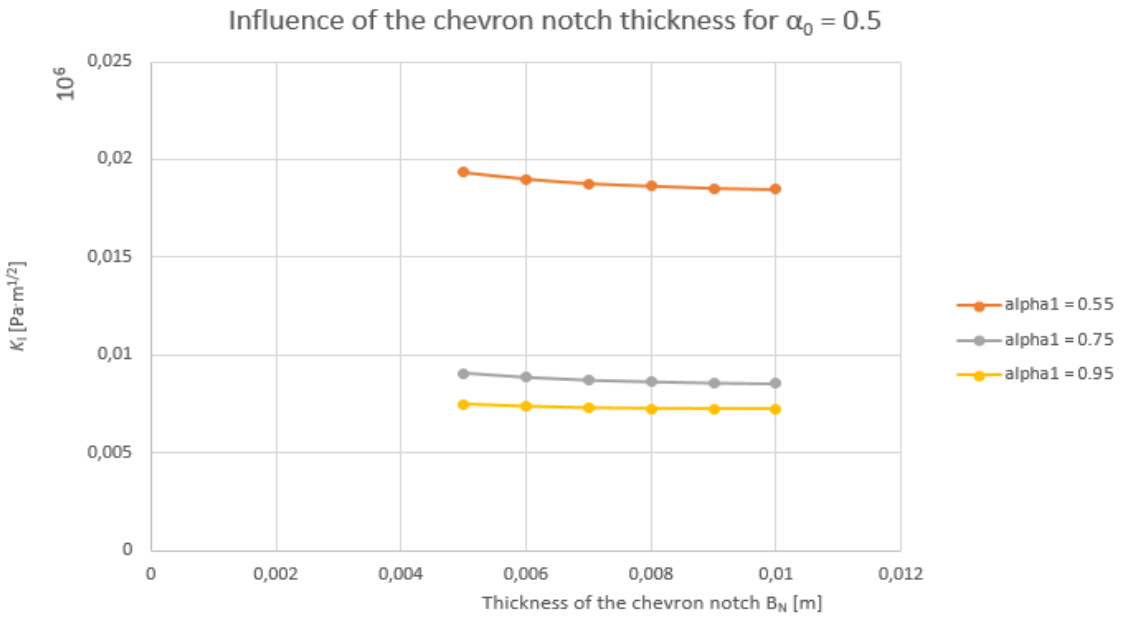

Figura 8 Influencia del espesor de la muesca chevron para diferentes valores de α_1 y α_0 = 0.5

El segundo sub-análisis se realizó de manera opuesta, es decir, para distintos valores de α_1 (constantes en cada caso), se fue estudiando que pasaba con el valor del factor de intensidad de tensiones para diferentes valores de α_0 dependiendo otra vez en el espesor de la muesca.

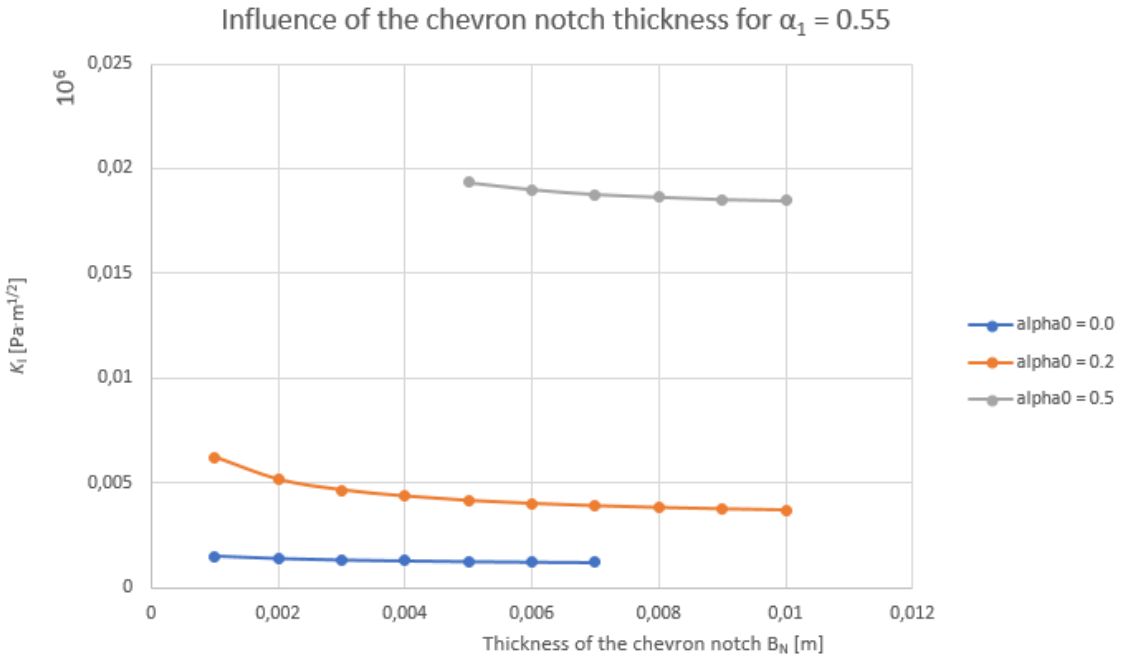

Figura 9. Influencia del espesor de la muesca chevron para diferentes valores de α_0 y α_1= 0.55

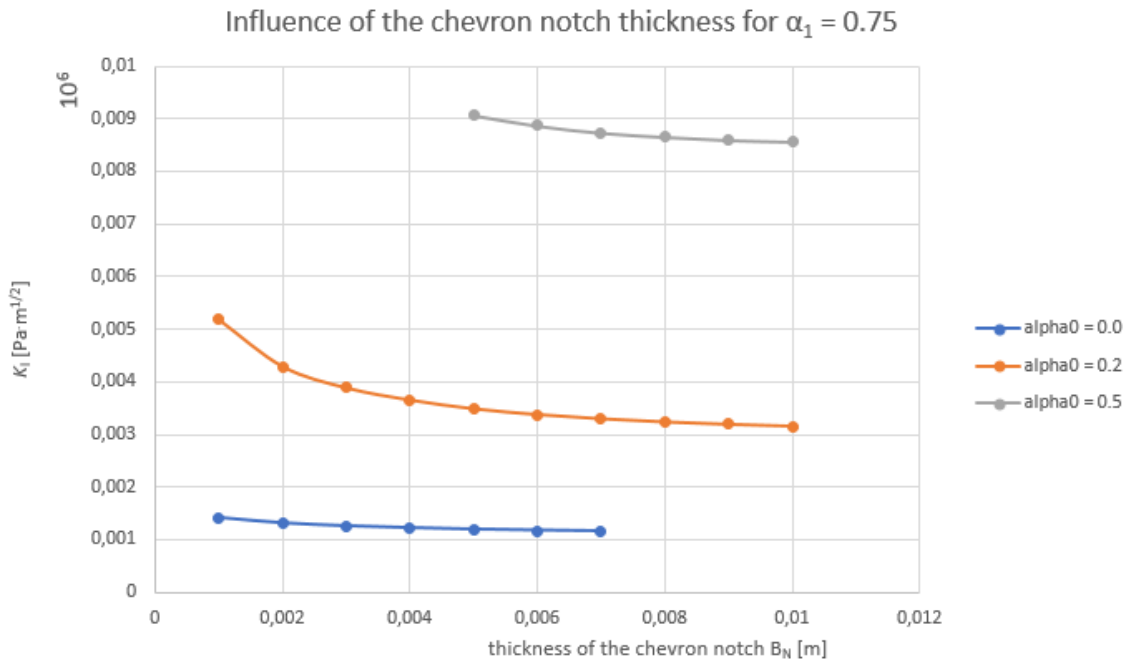

Figura 10 . Influencia del espesor de la muesca chevron para diferentes valores de α_0 y α_1= 0.75

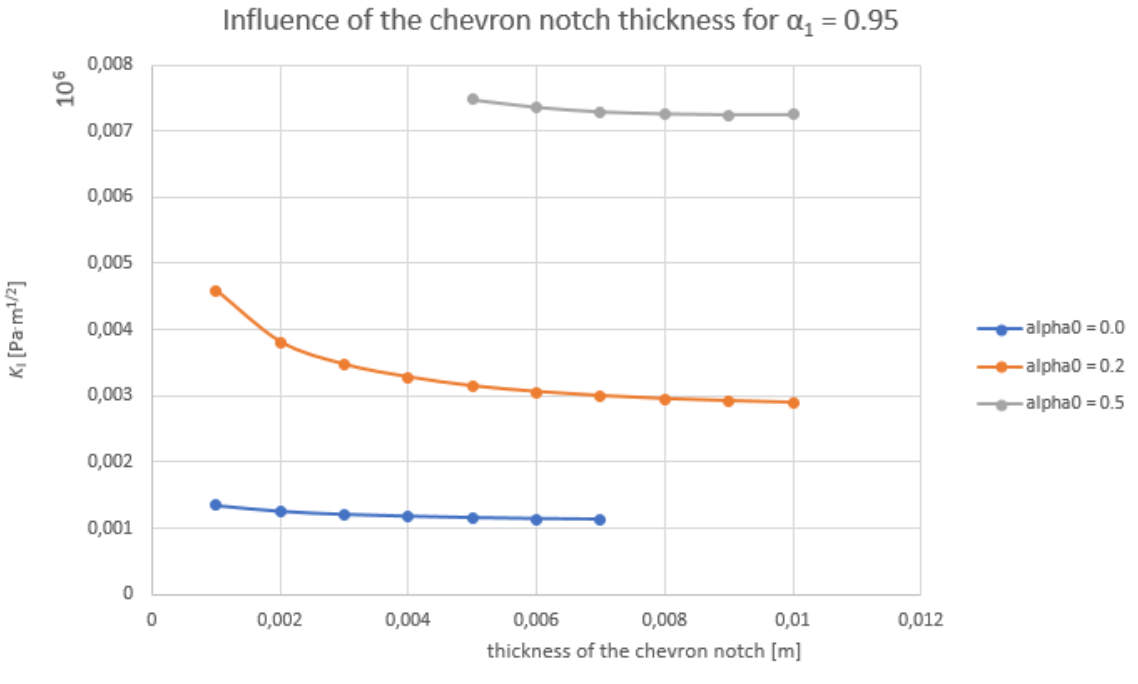

Figura 11. Influencia del espesor de la muesca chevron para diferentes valores de α_0 y α_1= 0.95

3.7 CONCLUSIONES

Influencia del número de capas utilizadas

Cómo se comentó previamente, para la realización de este estudio se utilizó la geometría 3PB de tal manera que utilizó la condición de tensión plana. A la vista de los resultados se recomienda la utilización de 7 capas o más para la resolución del modelo. El número óptimo de capas es 10 o más.

El modelo se realizó de tal manera que se pueden hacer posteriormente análisis paramétricos. Se podría por ejemplo cambiar la longitud inicial de la grieta, el ángulo de la muesca chevron la separación entre apoyos, etc.

Influencia del ángulo

Para la realización de este apartado se ha utilizado el Segundo tipo de geometría comentado es decir el correspondiente al 4PB. Se puede apreciar en los gráficos que el valor del factor de intensidad de tensiones es más estable para valores más altos del ángulo. También se puede ver que cuando se aumenta el valor del ángulo el valor de α_1 para el cual el factor de intensidad de tensiones cambia abruptamente es también más elevado. Se puede apreciar que la estabilidad del factor de intensidad de tensiones se mantiene siempre hasta que el valor de α_1 es igual al valor de α_0.

Influencia del espesor

Mirando las figuras correspondientes a este análisis, se puede apreciar que a medida que incrementamos el valor de α_0 el efecto del espesor (B_N) es más alto, esto significa que para valores más altos de α_0 la influencia del espesor es mucho mayor.

En la segunda parte del análisis se puede observar que para valores más pequeños del espesor el único valor de α_0 que tiene algo más de importancia en lo que se refiere al valor del factor de intensidad de tensiones es $\alpha_0 = 0.2$. También se puede ver que al aumentar el valor de α_1 manteniendo el valor del espesor y de α_0, el factor de intensidad de tensiones tiene un valor más pequeño.

4. Introduction

Our understanding of how materials can fail and our knowledge developed on how to prevent these failures have increased a lot during the recently years. There remain lots of things to be known but the advances on the field of fracture mechanics have helped to offset some potential dangers.

There are two main circumstances in which structural failures occur. The first one is during the stage of design, construction or operation of the structure. These can be due to human error or ignorance, also inappropriate analysis or lack of experience. The second one is more related with the application of new materials, it can derive on undesirable and unexpected behaviour. This type of failure is more difficult to prevent. The new material that is going to be used should be subjected to the appropriate testing to reduce the frequency of failures.

The field of fracture mechanics has prevented a big number of structural failures during the last years. When the criteria of this theory are applied in the correct way, not only helps to prevent the failures in the stages of design and behaviour, it also reduces the frequency of the failures due to the application of new materials. (Anderson, 2005).

In the design of modern engineering structures, it is required the proper determination of the fracture resistance of the materials with some parameter such as fracture toughness (K_{IC}) to fulfil the successful application of Linear elastic fracture mechanic's (LEFM).

In brittle materials (i.e. glass or structural ceramics) it is difficult to generate a sharp crack notch without fracturing the specimen. Chevron-notched specimen was developed to alleviate these problems produced as the result of the sharp starter cracks (M.G. Jenkins, et al., 1987).

As it is said in the title of this thesis, the theme that is going to be discussed is the use of chevron notch for the various test specimens. The reason of using this type of notch is due to all the advantages that are going to be explained in the whole document and to measure the length of the crack. Pre-cracked specimens are sometimes difficult to prepare, and the initial crack is sometimes not visible making more difficult to measure the crack length. To get over these difficulties Barker (L.M. Barker, 1979) has proposed a specimen with chevron notch, in which the crack originates at the tip of the triangular ligament during loading (Dietrich G. Munz, et al., 1980). The geometry of chevron notch presents an increasingly larger crack front to the advancing crack, thus forcing the crack to extend in a stable manner over the complete area of chevron notch. Therefore, energy principles, numerical methods, or empirical techniques may be applied to obtain the stress intensity factor of various chevron notched specimens (M.G. Jenkins, et al., 1987).

The chevron notched specimens are also used because of this shape facilitates the initiation of the fatigue pre-cracking. As it will be explained during the project, the properties of chevron notch are unique and can eliminate the need for pre-cracking (Anderson, 2005)

5. State of the art

5.1 HISTORY OF CHEVRON-NOTCHED SPECIMENS

To avoid the fracture when designing structures is not a new idea. It can be observed in the ancient Egypt pyramids or even in the Roman imperium. In Europe, there are buildings that were built in Renaissance period and are still being used for their original purpose. Prior to Isaac Newton the knowledge of mechanics was more limited, so the workable designs were probably achieved by trial and error. (Anderson, 2005).

Specimens with chevron notch were first used by Nakajama (J. Nakajama,1965). His configuration was used to measure fracture energy of brittle, polycrystalline, refractory materials.

Later, Tattersall and Tappin (H.G. Tattersall and G. Tappin,1966) proposed using a bend bar with a chevron notch symmetrical about the centre line of the specimen. This specimen was used to measure the work of fracture (determined from the area under the load-displacement divided by the area of the fracture surfaces) on different materials (J.C. Newman, 1984).

In 1972 Pook (Pook L.P., 1972) suggested using chevron-notched bar to determine the plane-strain fracture toughness of metals. However, he considered only the analytical treatment needed to obtain stress-intensity factors as a function of crack length for various types of chevron notches. He did not study the experimental aspects of using a chevron-notched specimen to obtain K_{IC} (J. C. Newman, 1984).

In 1975, Bluhm (J. Bluhm, 1975) analysed chevron-notched bend bars. He explained the difference between the straight-through crack and the one with chevron-notch using a slice model (D. Munz, 1980)

In 1978, Barker used the maximum load for fracture toughness and determined that for a given geometry of chevron-notched specimen, the crack length at maximum load will be independent of the test material (D. Munz, 1980).

Wu (Wu Shang-Xian ,1982) used equations to determine the stress intensity factors for three-point bending chevron-notched specimens. His results were almost the same as Pook (Pook L.P., 1972) suggested before.

In Figure 5.1 we can appreciate the different configurations of the specimens that have been explained above.

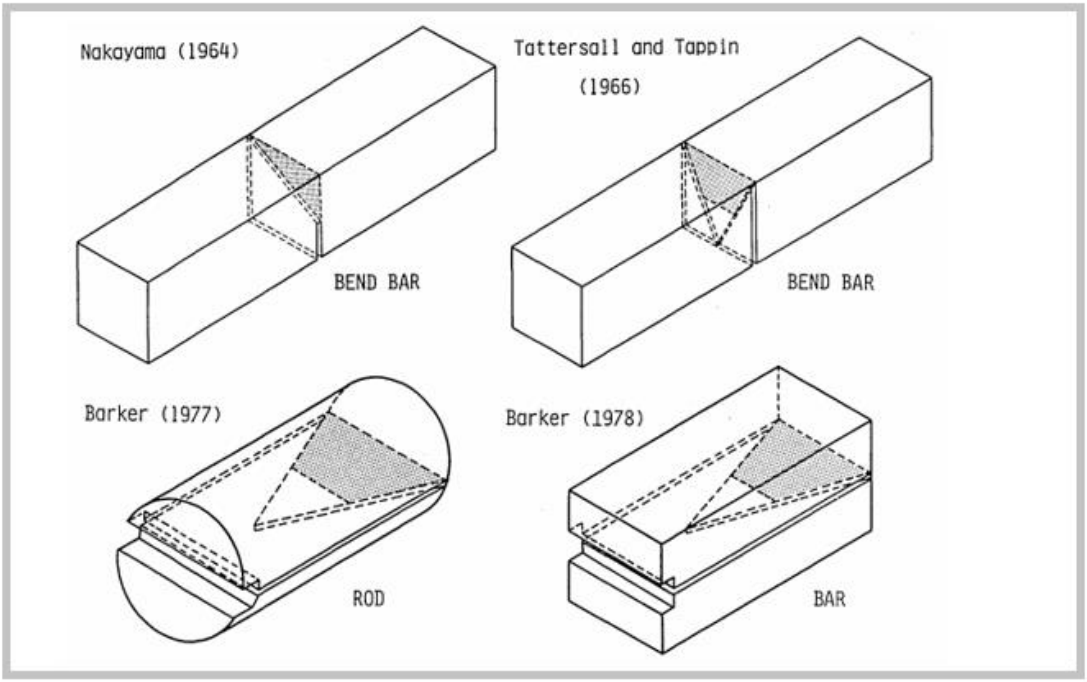

Figure 5. 1 Various chevron-notched fracture specimen configurations (J.C. Newman, 1984).

It is extremely important for a lot of applications, to be able to characterise the fracture behaviour of a current material. For this purpose, an accurate and sensitive testing method is necessary. The chevron-notched specimen technique is a well-established method used to determine the fracture toughness of brittle materials (A.R. Boccaccini, 2003).

5.2 GENERAL USAGE

Fracture mechanics plays often an important role in life prediction of components that are subjected to fatigue or stress corrosion cracking. The rate of cracking can be correlated with fracture mechanics parameters such as the stress-intensity factor (see section 7.4 in this document), and the critical crack size for failure can be computed if the fracture toughness is known.

For brittle materials (i.e. glasses and structural ceramics) it is difficult to generate a sharp crack in the specimen without fracturing it. One method that has been used lately with good results is to apply a thickness-wise compressive loading to the specimen while a wedge is gradually forced into the crack mouth opening (R.W. Davidge, 1970). While it is possible to produce very sharp initial cracks with this procedure, the method is time-consuming and sometimes when we are dealing with large number of test specimens the results can be inconsistent. One type of specimen that has emerged to solve the problems associated with producing this sharp start

cracks, is the chevron notched specimen. Newman (J.C. Newman, 1984) recently reviewed the development of this specimen from 1964 to the present (M.G. Jenkins, et al., 1987).

Destructive tests specimens of quasi-brittle materials subjected to 3PB test are becoming a very common way of testing some building structures and its parts. This kind of tests are usually accompanied by stress concentrators (i.e. chevron-notch) to make the crack propagation to be directly in the central plane of the test specimen (J.C. Newman, 1984).

In the figure below we can appreciate a schema of a test specimen with an initial chevron notch:

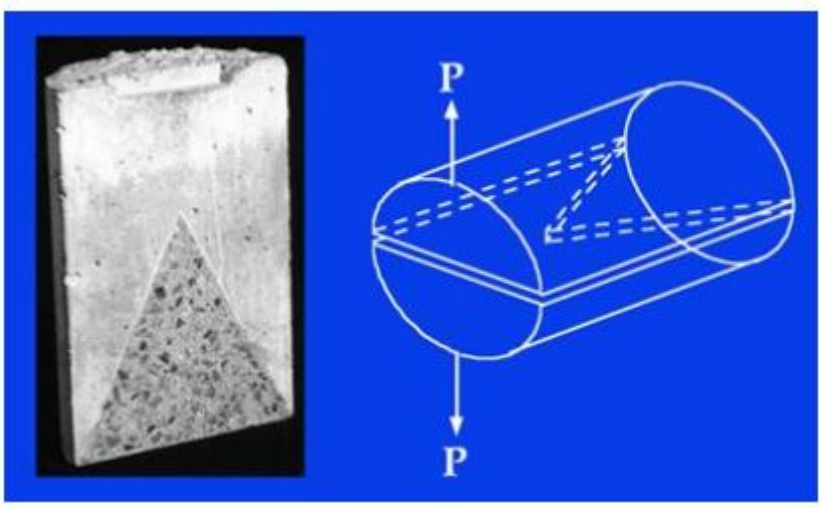

Figure 5. 2 Schema of test specimen with an initial chevron notch (adopted from: http://www.lmc.ep.usp.br/people/umberto/research/sr1-i.html)

The plane-strain fracture toughness, K_{IC}, of brittle materials can be obtained using a short bar specimen with a chevron notch. The advantage of this specimen type is that a sharp natural crack is produced during loading (D.Munz, et al., 1980), this means that there is no pre-cracking required. Because of this, chevron-notched specimens are also suited as quality control specimens (J.C. Newman, 1984)

The load reaches a maximum at a constant material-independent crack length-to-width ratio for a specific geometry.

In comparison with the conventional fracture toughness specimens, the chevron-notched ones have some features to be mentioned:

- High stress concentration at the tip of the chevron notch. Therefore, the crack initiates at a low applied load (pre-cracking is not needed)
- Stress intensity factor passes through a minimum as the crack grows

Because of these features, some of these specimens are being considered for standardization by the American Society for Testing and Materials (ASTM) (J.C. Newman, 1984).

Many investigators have made studies about the advantages and disadvantages of using chevron-notched specimens for determination of plane-strain fracture toughness of brittle materials. Some of these are summarized here: (J.C. Newman, 1984).

Advantages:

- Small specimens
- No need of fatigue pre-cracking
- Simple procedure
- High constraint at a crack point
- Notch guides crack path

Disadvantages:

- Restricted to brittle materials
- Thickness limitation (less than 5 mm is difficult to test)

6. Aim

In this project, it´s going to be explained a numerical analysis done with ANSYS (for proper description of solved problem) numerical system for test specimens with initial chevron notch. For this type of analysis, the calculation of stress intensity factor is crucial. To achieve this, the first step was to look for all the information about this topic in scientific articles and books in the web and library.

This thesis is focused on the creation of a 2D numerical model with different input parameters (i.e. the number of layers (*N*), geometry, material models, different boundary conditions). This 2D model was created in a way in which the input parameters are generated by the model itself by proper macro file. Also, it is going to be evaluated how the value of the stress intensity factor changes according to the different values of the input parameters.

7. Theoretical background

7.1 LOADING MODES

There are three basic loading modes in which the crack can grow depending on the orientation of the crack respect to the direction of the applied load:

- Mode I: it is also called opening mode. This is the case used in this document. The predominant stress for this mode is σ_{YY}
- Mode II: it is also called displacement mode or in-plane shear. For this mode, the predominant stress is τ_{YX}
- Mode III: it is also called out-of-plane shear. The predominant stress is τ_{YZ}

The most common is the first mode. In Figure 7. 1 we can appreciate the three loading modes:

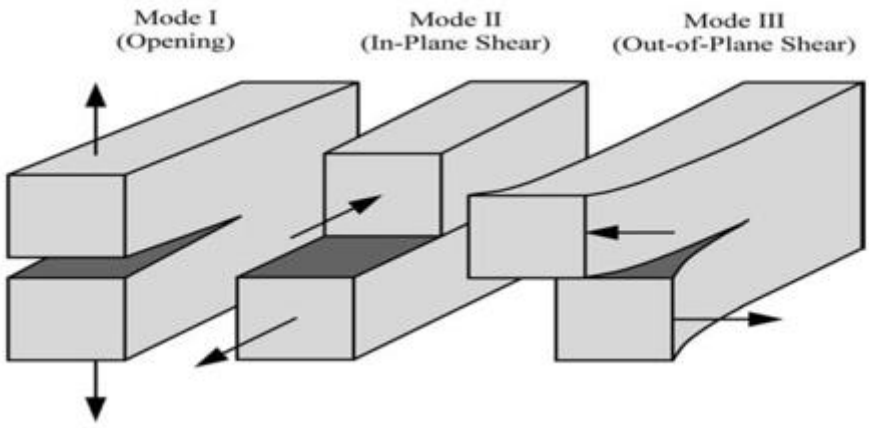

Figure 7. 1 Different loading modes depending on the orientation of the crack respect to the direction of the applied load. (Anderson, 2005)

Each mode produces the singularity at the crack tip, but the proportionality constants *K* depend on the mode. *K* is the stress intensity factor which will be explained in the section 7.4 of this document. This *K* factor is usually given a subscript to denote the mode of loading (K_I, K_{II}, K_{III}).

Mode I is not only the most common, it is also quite simple. The crack will propagate when the stress intensity factor reaches a certain critical value K_{IC} (fracture toughness for the given material).

With this definition, the local fracture criterion for pure mode I could be explained as:

If $K_I < K_{IC}$ then no crack growth (stable)

If $K_I = K_{IC}$ then quasi-static growth possible

If $K_I > K_{IC}$ then dynamic growth (unstable)

If the loadings applied are not pure mode I, the problem becomes more difficult because, in general, not only the loading combination is needed, but also the kink direction. This is still an open problem today. (Bažant, 1984)

7.2 LINEAR ELASTIC FRACTURE MECHANICS

Fracture mechanics is the field of mechanics, which is focused on the study of the propagation of cracks in the materials. Analytical methods of solid mechanics are used to calculate the force on a crack and later with experiments characterize the material resistance to fracture. The are many essays that show how the stresses around a corner or a hole in a stressed plate can be many times higher than the average applied stress. When a concentrated stress exceeds the material´s theoretical value of cohesive strength the crack can propagate and the material can fail.

To define what is linear elastic fracture mechanics first it should be defined what is fracture and what types of fracture exist depending on the deformation produced.

Fracture can be defined as the separation of a solid in two or more parts because of tensions. There clearly exist three types of fracture (Figure 7.2):

- Brittle: it is characterized by the separation of the material in a plane perpendicular to the direction in which the load is being applied and with the absence of plastic deformation. The brittle material (i.e. glass) shows a linear elastic behaviour almost up to the peak load, and the crack will propagate through the specimen just after the peak.

- Quasi-brittle: For these types of materials (i.e. concrete and some ceramics), the non-linear behaviour starts before the peak load and then upon arrival at the peak load the crack will start to propagate.

- Ductile: This kind of material present an important previous plastic deformation so the fracture takes place on a distorted zone. In this case, the plastic dissipation energy is much greater than the elastic energy, that is why the crack growth is governed by the plastic work. The non-linear behaviour starts much more before the crack localization. (Shailendra Kumar & Udhirkumar V. Barai ,2011).

In the next figure, we can observe the behaviour of these three types of materials. It is represented the stress displacement behaviour under uniaxial tension for brittle, quasi-brittle and ductile materials.

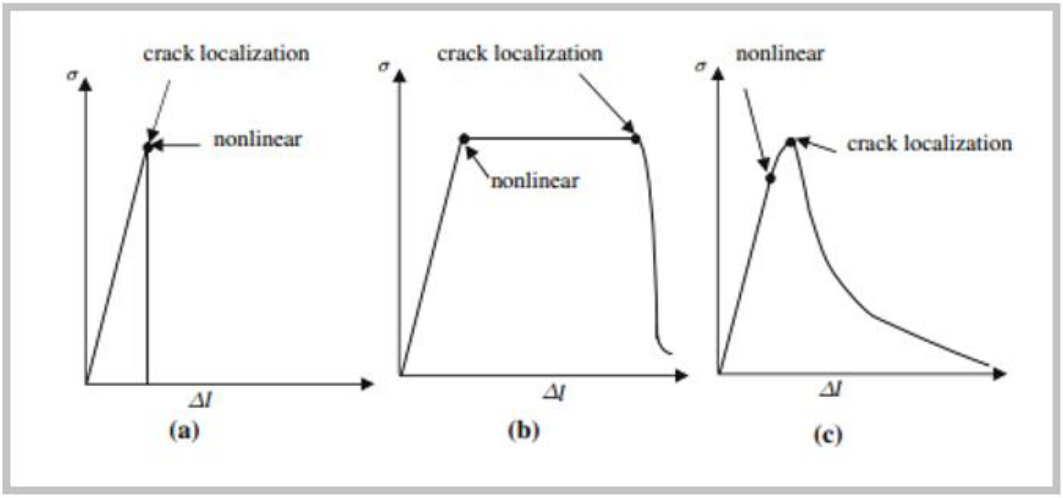

Figure 7. 2 Stress-strain behaviour under uniaxial tension (a) brittle materials, (b) ductile materials, (c) quasi-brittle materials (Shailendra Kumar & Udhirkumar V. Barai ,2011)

The assumptions made for Linear Elastic Fracture Mechanics are:

- Isotropic material: this means that the material has identical value properties in all directions. This property is important because the sensitivity to orientation in particularly pronounced in fracture toughness measurements (microstructure with a preferred orientation may contain planes of weakness, where the crack propagation is relatively easy). (Anderson, 2005)

- Linear elastic material: this means that the applied stress is linearly proportional to the obtained strain.

Based on these assumptions the stress near the crack tip can be calculated by using the theory of elasticity. When the stresses near the crack tip exceed the material fracture toughness, the crack will grow. These assumptions are also valid if the deformation is small compared to the size of the crack (small-scale yielding), in other cases (large zone of plastic deformation) the Elastic Plastic Fracture Mechanics (EPFM) must be used.

Fracture mechanics theories have been developed also for nonlinear material behaviour (i.e. plasticity and viscoplasticity) as well as dynamic effects. However, all these effects are extensions of the linear elastic fracture mechanics (LEFM). This theory is valid only if nonlinear material deformation is confined to a small region surrounding the crack tip. In many materials, it is virtually impossible to characterize the fracture behaviour with LEFM, and an alternative fracture mechanics model is required (Anderson, 2005). In the Figure 7.3 it can be observed what it has been explained above:

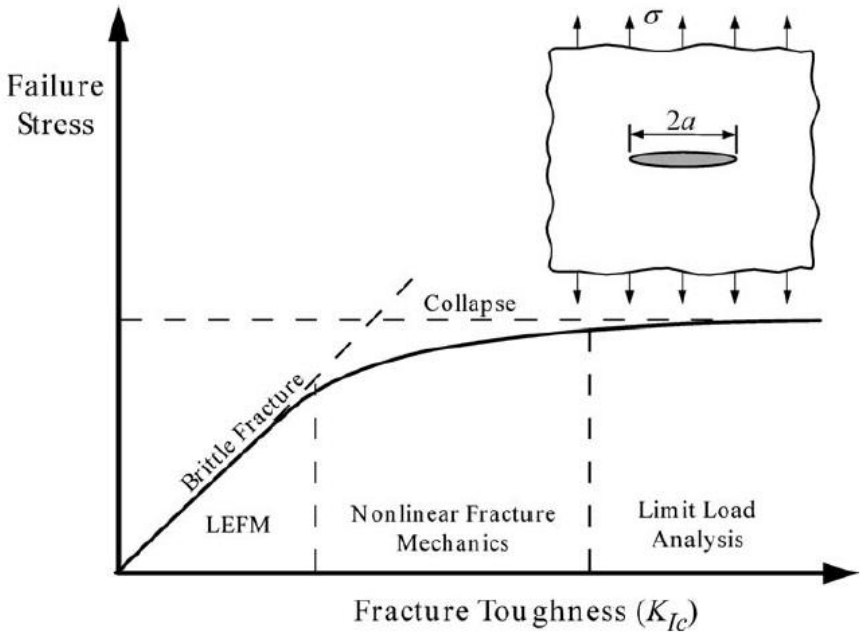

Figure 7. 3 Effect of fracture toughness on the governing failure mechanism (Anderson, 2005)

Most of the materials contain small cracks or contaminants (i.e. foreign particles) that concentrate the stress, that's why the real fracture strength of a material is always lower than the theoretical value. These defects concentrate the stress, removing them increases the strength (Fischer Cripps, 2007).

7.3 WILLIAMS EXPANSION

The Williams expansion is a power series, it is intended to estimate the extent of the non-linear zone (called Fracture process zone - FPZ), which plays a significant role in the failure of non-brittle materials. Considering that in the case of elastic-plastic and quasi-brittle materials the size of this zone is substantial compared with the specimen dimensions, it is necessary to consider a big region around the crack tip (V. Veselý et al., 2014)

A variety of techniques are available for analysing stresses in cracked bodies. The Williams approach considers the local crack-tip fields under generalized in plane loading (Anderson, 2005).

The Williams approach uses the multiparametric fracture mechanic to describe the stress field in the crack tip (Williams, 1957). For a two-dimensional homogeneous elastic isotropic body with a crack subjected to mode I of loading, the stress and displacement fields can be expressed in the form of an infinite power series, the Williams expansion (Williams, 1957). For the stress tensor $\{\sigma\}$ and the displacement vector $\{u\}$, we have the next equations:

$$\begin{Bmatrix}\sigma_x\\ \sigma_y\\ \tau_{xy}\end{Bmatrix} = \sum_{n=1}^{\infty} \frac{n}{2} r^{\frac{n}{2}-1} A_n \cdot \begin{Bmatrix}\left[2+(-1)^n+\frac{n}{2}\right]\cos\left(\frac{n}{2}-1\right)\theta - \left(\frac{n}{2}-1\right)\cos\left(\frac{n}{2}-3\right)\theta \\ \left[2-(-1)^n-\frac{n}{2}\right]\cos\left(\frac{n}{2}-1\right)\theta + \left(\frac{n}{2}-1\right)\cos\left(\frac{n}{2}-3\right)\theta \\ -\left[(-1)^n+\frac{n}{2}\right]\sin\left(\frac{n}{2}-1\right)\theta + \left(\frac{n}{2}-1\right)\sin\left(\frac{n}{2}-3\right)\theta\end{Bmatrix} \quad 7.1$$

$$\begin{Bmatrix}u\\ v\end{Bmatrix} = \sum_{n=1}^{\infty} \frac{r^{n/2}}{2\mu} A_n \cdot \begin{Bmatrix}\left(k+\frac{n}{2}+(-1)^n\right)\cos\frac{n}{2}\,\theta - \frac{n}{2}\cos\left(\frac{n}{2}-2\right)\theta \\ \left(k+\frac{n}{2}-(-1)^n\right)\sin\frac{n}{2}\,\theta + \frac{n}{2}\sin\left(\frac{n}{2}-2\right)\theta\end{Bmatrix} \quad 7.2$$

In these equations, r and ϑ are polar coordinates with origin centered on the crack tip (see Figure 6.4). The parameter n represents the index of the term of the power expansion. The coefficient μ is the shear modulus (see equation 6.3) and k is the Kolosov´s constant (see equations 7.4 and 7.5)

$$\mu = \frac{E}{2(1+\upsilon)} \quad 7.3$$

$$k = \frac{3+\upsilon}{1+\upsilon}\ ; PLANE\ STRESS \quad 7.4$$

$$k = 3-4\upsilon\ ; PLANE\ STRAIN \quad 7.4$$

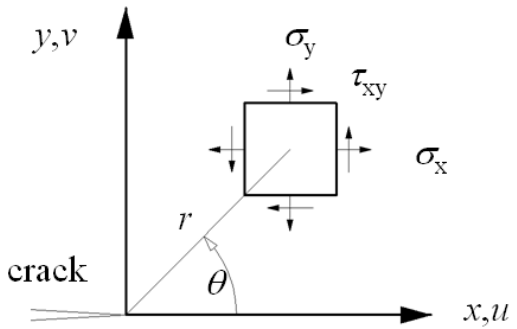

Figure 7. 4 Coordinate polar system at the crack tip. Considering crack propagation along the positive *x*-axis (Veselý,2004)

7.4 STRESS INTENSITY FACTOR

The stress intensity factor is a constant which characterizes completely the crack tip conditions in a linear elastic material. If this constant is known, the entire stress distribution at the crack tip can be computed (Anderson, 2005)

It should be considered that the term stress intensity factor is different from the term stress concentration factor. The second one is used to characterize the ratio between actual and average or nominal stress at a geometric discontinuity while the stress intensity factor defines the amplitude of the crack-tip singularity (Shailendra Kumar & Udhirkumar V. Barai,2011).

Let´s consider an arbitrary component with and arbitrary geometry and size of crack with an applied load as mode I. The field of stress in any point situated in the surroundings of the crack will be:

$$\sigma_Y = \frac{K}{\sqrt{2\pi r}} \cos\frac{\theta}{2}\left(1 + \sin\frac{\theta}{2} - \sin\frac{3\theta}{2}\right) \qquad 7.5$$

$$\sigma_X = \frac{K}{\sqrt{2\pi r}} \cos\frac{\theta}{2}\left(1 - \sin\frac{\theta}{2} - \sin\frac{3\theta}{2}\right) \qquad 7.6$$

$$\tau_{XY} = \frac{K}{\sqrt{2\pi r}} \cos\frac{\theta}{2} \sin\frac{\theta}{2}\cos\frac{\theta}{2} \qquad 7.8$$

All these expressions are valid for any geometry and type of load, this implies that the tensions surrounding the front crack (σ_X, σ_Y, τ_{XY}) are only dependant on *K*, it is known as stress intensity

factor and it characterises the tensional state surrounding the crack (Francisco Javier Belzunce Varela, 2014).

This parameter *K*, regulates the entire tensional level at any point in the front of the crack. Therefore, crack advance and material rupture will occur when this factor reaches a constant critical value characteristic of each material, denominated fracture toughness (K_C).

For complex situations, the stress intensity factor can be estimated by experiment or numerical analysis.

7.5 FRACTURE TOUGHNESS

To measure the resistance of a material to crack extension the fracture toughness tests are done (Anderson, 2005). To understand better this section, it is recommended to read first the section 6.4 in which it is explained what is the stress intensity factor. If it is assumed that the material fails at some critical combination of stress and strain, then the fracture must occur at a critical value of the stress intensity K_{IC}, this is an alternate measure of fracture toughness.

For the case of the chevron-notched specimens, the fracture toughness may be expresses as:

$$K_{IC} = A \cdot P_{MAX} \qquad 6.8$$

Where P_{MAX} is the maximum test load, and the coefficient *A* is dependent on the geometry of the specimen and the manner of loading (D. Munz, 1980). Later this *A* was replaced by the dimensionless shape function *Y* and the nominal stress in the centre plane of the specimen.

7.6 THREE POINT BENDING TEST

The three-point bending test consists of a sample which is placed on two supporting pins and loaded. For the case of this project it is going to be used the three-point bending test for one of the analysis done, as it is shown in the figure below:

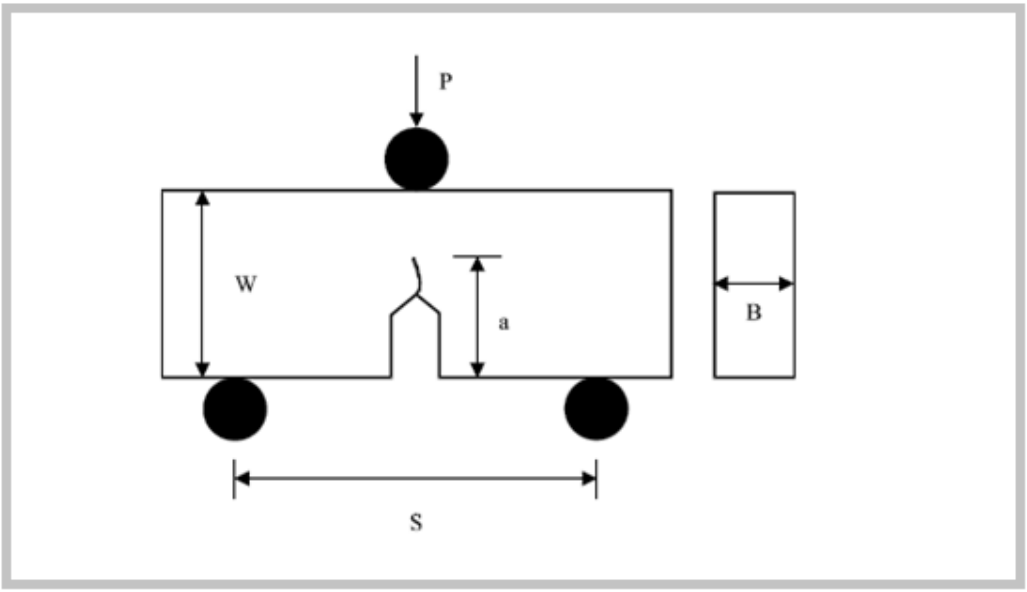

Figure 7. 5 Three-point bending test (Francisco Javier Belzunce Varela, 2014)

For the figure above the parameters used are:

a → crack length [m]

B→ thickness of the specimen [m]

P→ Peak load taken from loading diagram [N]

S → distance between supports [m]

W → width of the specimen [m]

This type of test produces tensile stress in the convex side of the specimen and compression stress in the concave side. Because of this, an area of shear stress is produced along the midline.

The advantage of using this type of test is the ease of the specimen preparation and testing. The disadvantage is that the results of the testing method are sensitive to specimen and loading geometry and strain rate (boundary conditions).

7.7 FOUR POINT BENDING TEST

In Figure 7.6 we can appreciate a basic scheme of how a 4PB test would be. The specimen is placed in two suppoting pins. Two loads are applied at the same distance from the center of the specimen.

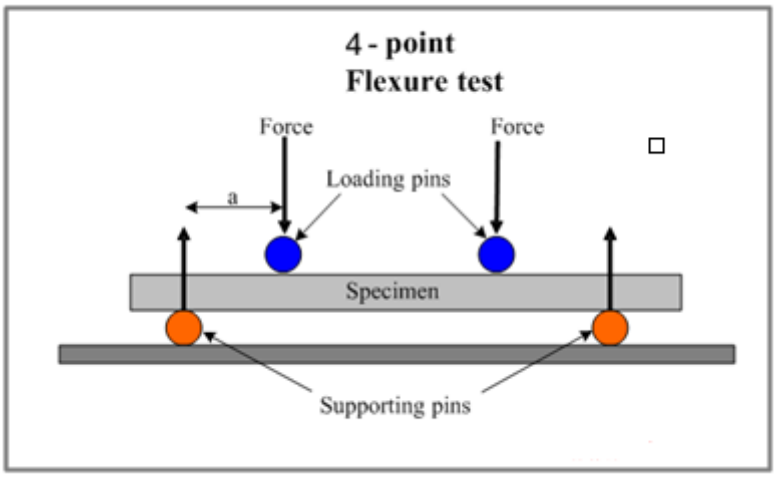

Figure 7. 6 Four-point bending test (www.substech.com)

This test is very similar to the three-point bending test, which was explained in the previous paragraph. The major difference between 3PB test and 4PB test is that in the second case there is a larger portion of the beam subjected to the maximum stress. This means that the volume under stress is bigger in 4PB test than in 3PB test. If the Weibull statics are considered, the mechanical strength expected in 4PB test would be lower than the one in 3PB test. According to Weibull statics, if the volume is bigger, the probability of finding longer cracks is higher in general (https:// www.researchgate.net).

8. Numerical model

8.1 CREATION OF THE MODEL

As it is said in the beginning of this project, the numerical model was developed using FE software ANSYS. This is an engineering simulation software that helps to solve complex design challenges (adopted from: http://www.ansys.com/).

Only the symmetrical half of the specimen's body was used with the plane stress condition – the reason was to simulate the non-uniform thickness of the notch layer along the height of the cross section.

To start with the creation of the model the first step is to have an idea of what exactly is going to be modelled in the program. The Figure 8.1 and 8.2 show the geometries that were used for this project. Below, in this same section we can find the dimensions that were used for those parameters represented in the schemes. In the first one it is represented the 3PB test and in the second one the 4PB test.

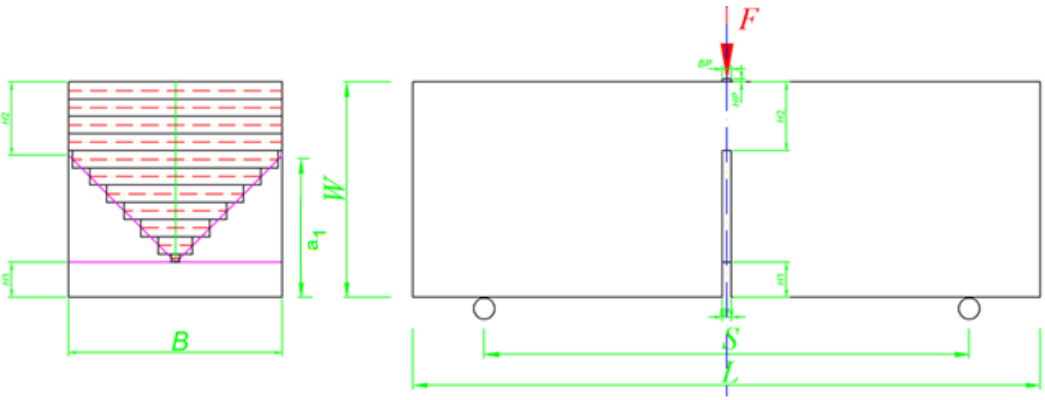

Figure 8. 1 Geometry of the 3PB test specimen configuration with initial chevron notch. (J. Sobek, et al.,2017)

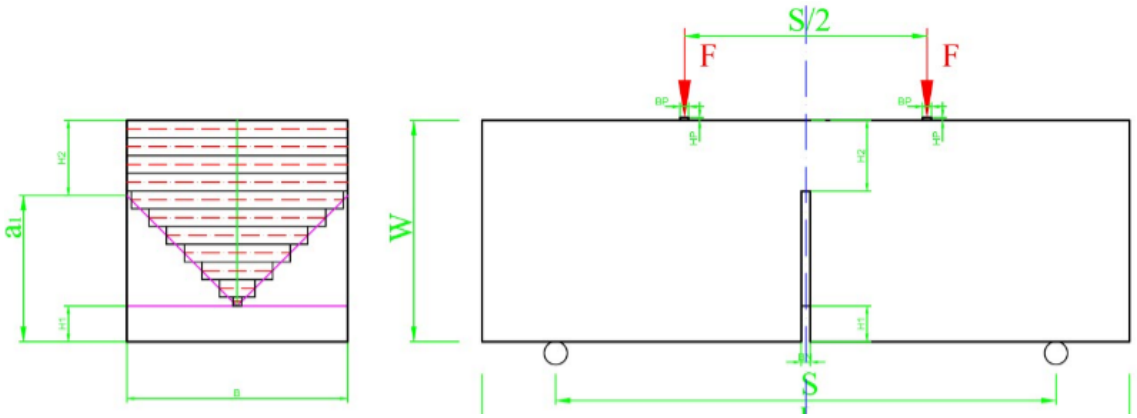

Figure 8. 2 Geometry of the 4PB test specimen configuration with initial chevron notch.

The parameters used in these schemes are:

a_1 → Parameter which characterizes the ending of the linear function of the chevron notch measured from the bottom part of the test specimen [m]

B → Thickness of the specimen [m]

B_N → Thickness of chevron notch [m]

B_P → Thickness of the steel part [m]

F → Force applied into the test specimen [N]

H_1 → Initial crack length [m]

H_2 → Distance from the end of the specimen to the beginning of the crack [m]

H_P → Width of the loading platen [m]

L → Length of the specimen [m]

S → Span of supports [m]

W → Width of the specimen [m]

For the implementation of this project two types of geometry were used. The first one correspond to the 3PB test and the parameter used for this geometry were:

W = 0.1 m; B = 0.1 m; L = 0.4 m; S = 0.36 m; B_N = 0.003 m; N (changeable)

The second geometry used is the one that correspond with the 4PB test and the parameters used in this case were:

W = 0.1 m; B = 0.1 m; L = 0.825 m; S = 0.8 m; B_N (changeable); N = 30

Once we have clear the model that is going to be used we can introduce it in ANSYS. The code that was introduced in ANSYS is structured in different parts. To see exactly how does the code look, go to the Appendix of this document.

First, we define the parameters that are going to be used. In this case, we wanted some of these to be changing (and study the variation of the results depending on its value) so the creation of loops was needed.

Next step was the definition of the element type and the material, in the sections 7.2 and 7.3 it is explained with more details. In our case as it is a 2D plane model the *PLANE82* (2D 8-node structural solid element) was used. Once we have the element type we insert the key points (*KP*). Once we have the key points we need to create the areas so we can later mesh it. In this case. The command *KSCON* was used to consider the stress singularity at the crack tip.

Once we have all this, the next step is to mesh the geometry. We also need to define two meshes, one for the concrete and the other one for the steel part. The last step before solving and obtaining the results is the definition of the boundary conditions. In this case, we have the usual ones that correspond to a three-point bending test and four-point bending test. This means vertical and horizontal components of the applied load, fixed nodes in both directions of the support.

The last step is the calculation to obtain the results. For this, as we are making a model in which the parameters are generated by the model itself we decided to create a document (txt file) in which all these changes were summarized.

From figure 8.3 to figure 8.10 which are shown below it can be appreciated different configurations of the 3PB test with initial chevron notch depending on the values of H_1(initial crack length) and H_2 (distance from the end of the specimen to the beginning of the crack).

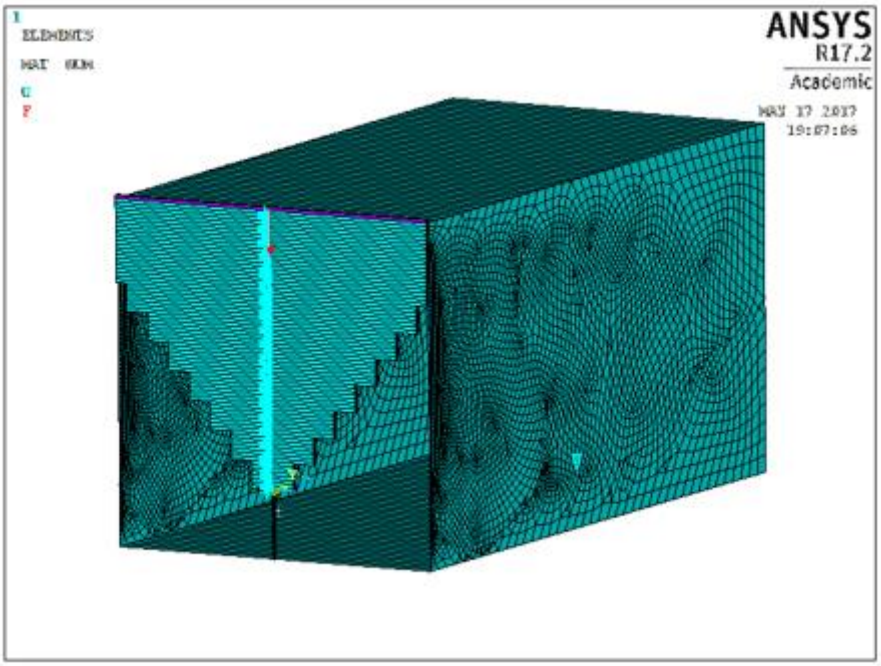

Figure 8. 3 Three-point bending test for H_1 = 0.02 and H_2 = 0.02

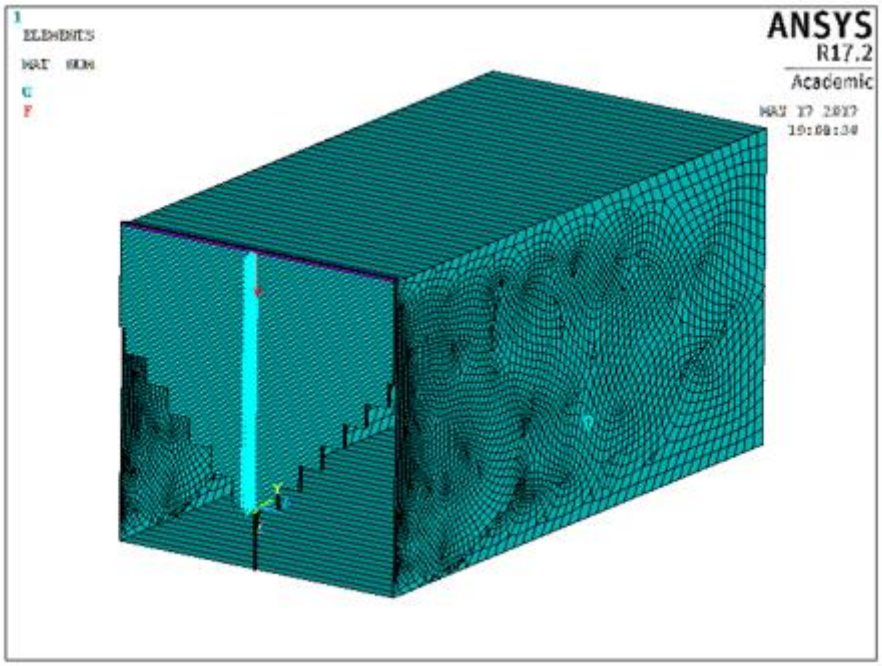

Figure 8. 4 Three-point bending test for $H_1 = 0.02$ and $H_2 = 0.03$

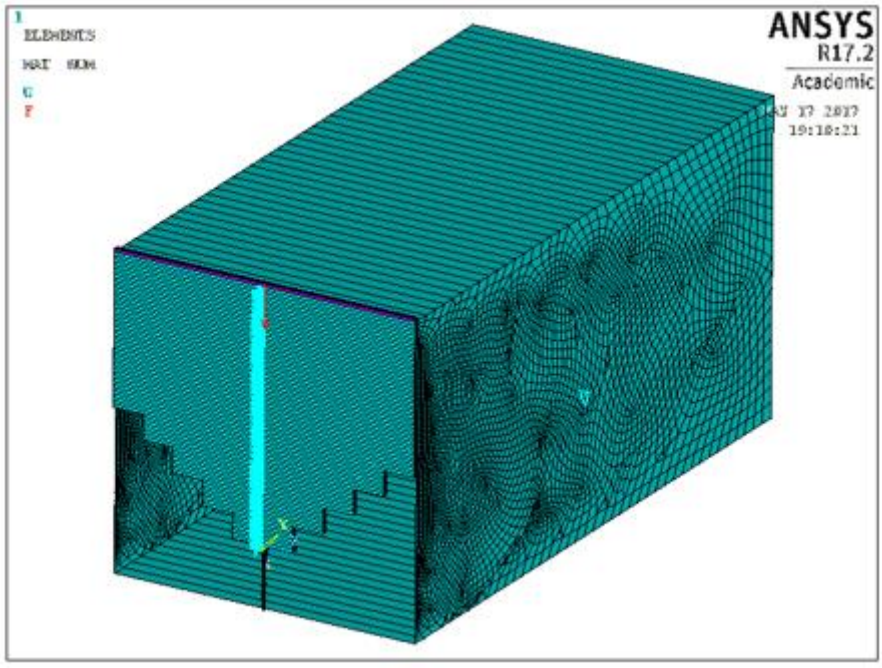

Figure 8. 5 Three-point bending test for $H_1 = 0.02$ and $H_2 = 0.04$

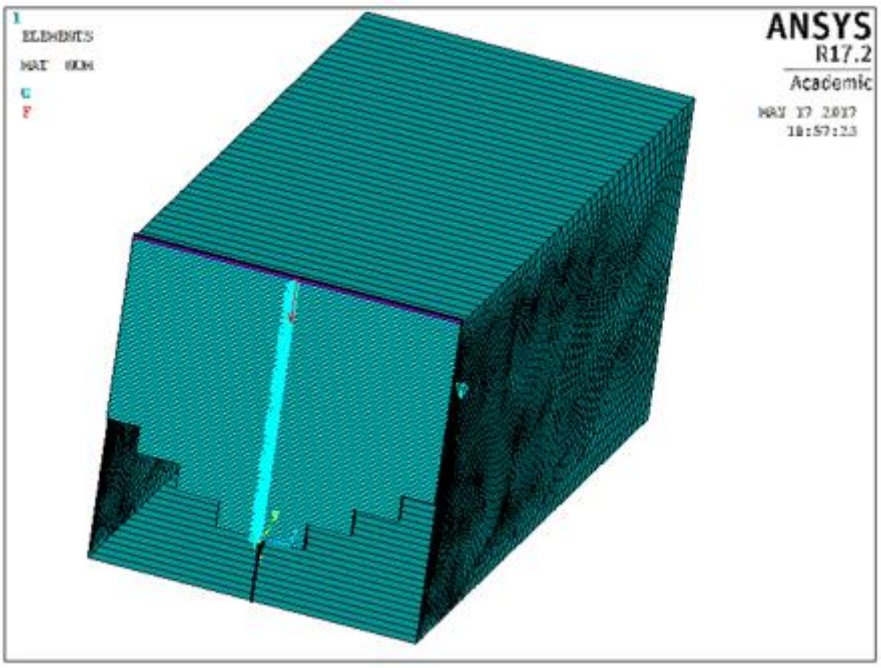

Figure 8. 6 Three-point bending test for $H_1 = 0.02$ and $H_2 = 0.05$

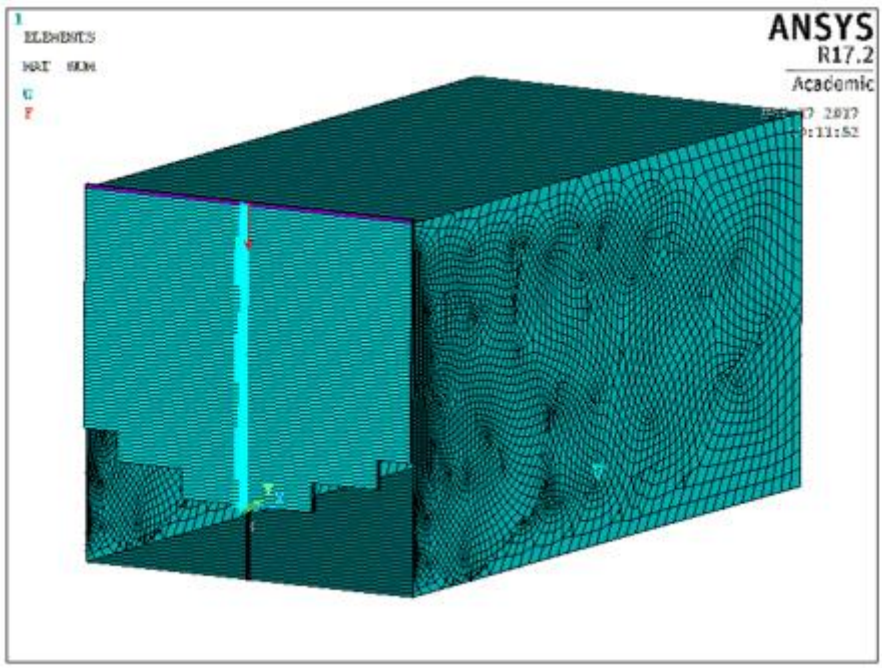

Figure 8. 7 Three-point bending test for $H_1 = 0.02$ and $H_2 = 0.06$

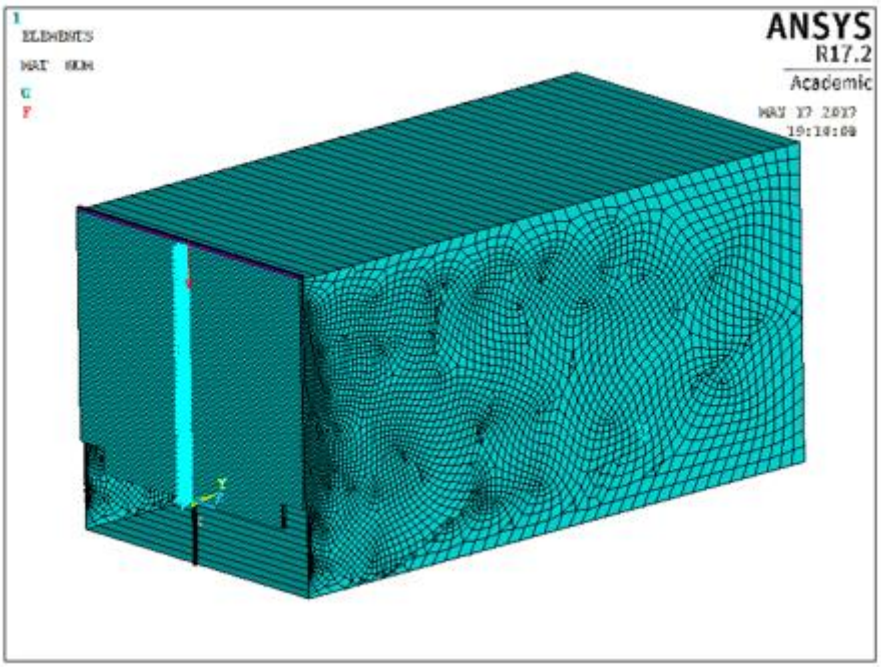

Figure 8. 8 Three-point bending test for $H_1 = 0.02$ and $H_2 = 0.07$

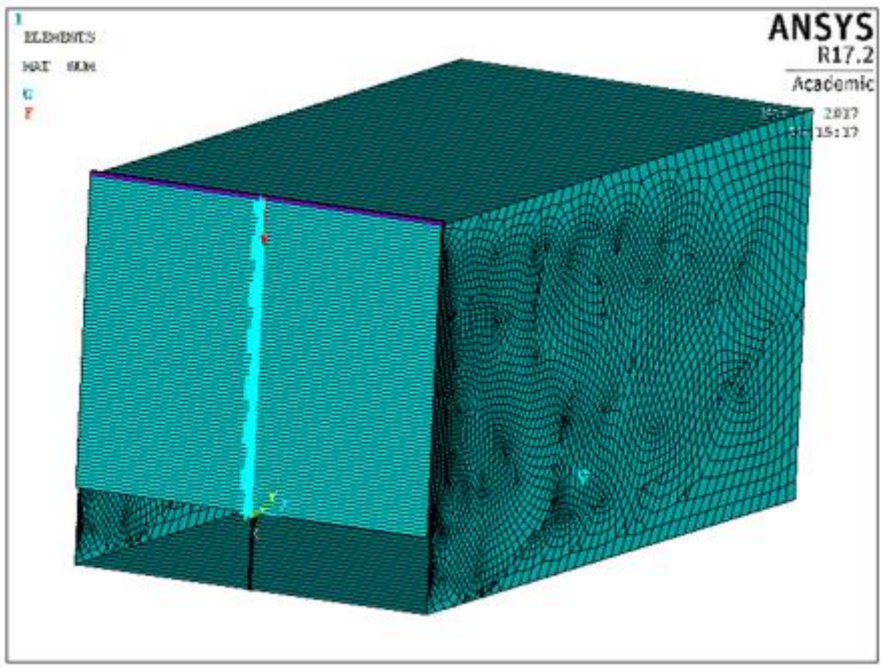

Figure 8. 9 Three-point bending test for $H_1 = 0.02$ and $H_2 = 0.08$

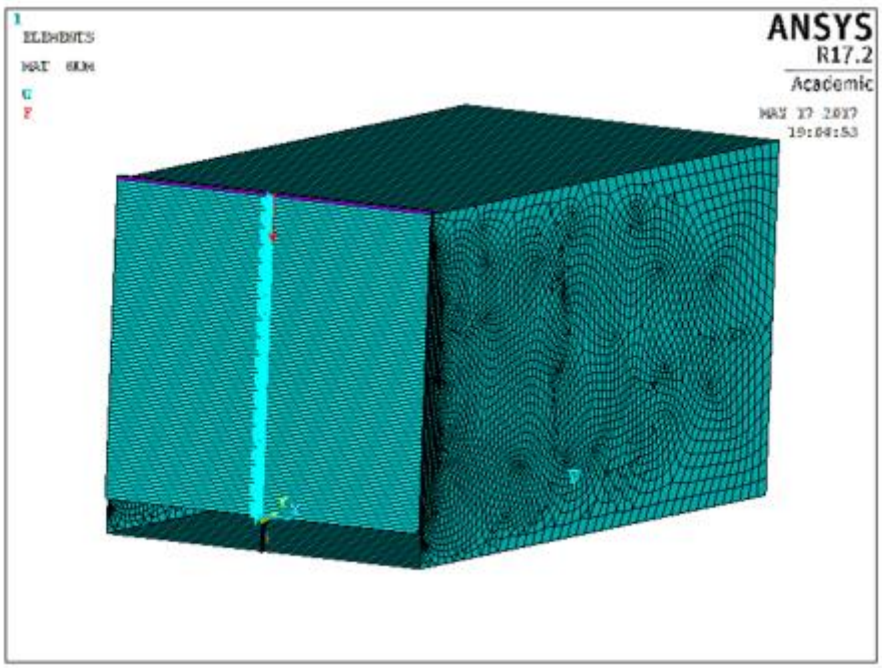

Figure 8. 10 Three-point bending test for $H_1 = 0.02$ and $H_2 = 0.09$

As it is appreciated in the figures above, if the value of H_1 remains constant (in this case equal to 0.02) as we increase the value of H_2 from 0.2 to 0.9 the chevron notch loses the characteristic V-shape.

Below in Figure 7.11 we can see two examples for the four-point bending test in which it is also appreciated the difference of the V-shape depending on the parameters H_1 and H_2.

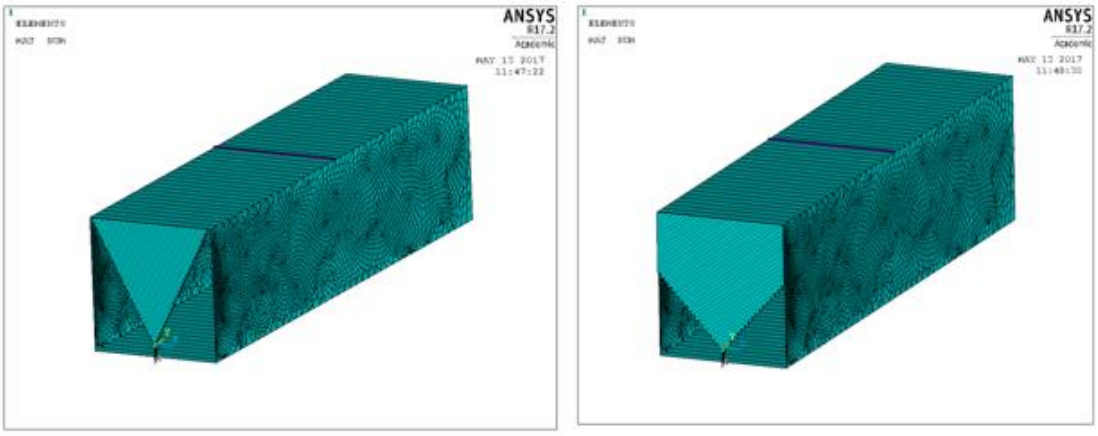

Figure 8. 11 Four- point bending test. In the left—characteristic V-shape for chevron notch. In the right—other combination of H_1 and H_2 values

8.2 MATERIAL PROPERTIES OF 3PB TEST

The test specimen is made from quasi-brittle material, in this case concrete with modulus of elasticity E = 35 GPa and Poisson's ratio v = 0.2. The loading platens are fabricated from steel with modulus of elasticity E = 210 GPa and Poisson´s ratio v = 0.3. The value of the force applied (F) is equal to 1000 N for all the cases of 3PB usage

In this case, there are two element types created. One just created for the loading platens and the other is used for the rest of the model.

8.3 MATERIAL PROPERTIES OF 4PB TEST

The test specimen is made from ductile material, in this case aluminium with modulus of elasticity E = 72.3948 GPa and Poisson's ratio v = 0.3. The loading platens are fabricated from steel with modulus of elasticity E = 210 GPa and Poisson´s ratio v = 0.3. The value of the force applied (F) is equal to 100 N for all the cases of 4PB usage.

9. Results and Discussions

9.1 IMPACT OF THE NUMBER OF LAYERS USED

To obtain the values of the stress intensity factor, the command *KCALC* was used. The calculations were done by changing the values of the parameters so we can study the different results obtained. To check the functionality of the model, it was compared with the 3PB test configuration with classical initial notch on the form of straight line.

To make this study it was taken N with the values of 3, 5, 7, 9, and 10. Also it must be considered that he parameter H_1 (initial crack length) is dependent on the maximum relative crack length H_2 (solid part of the cross section in the direction of the chevron notch).

Below, in Figure 8.1 we can appreciate how K_I is dependant of H_1 for a fixed value of H_2 (in this case it was chosen the value 0.5 for this parameter — this means half of the width of the test specimen). In this figure, we can appreciate two important things:

- The values of K_I are stabilized when the number of layers used is higher than 7. Between N = 9 and N = 10 the difference is practically negligible.
- With the division of the cross-section into three layers, there is an instability in study crack interval of K_I progress and against N = 10 the last value is three times larger. Similar deviation can be observed in the case of N = 5.

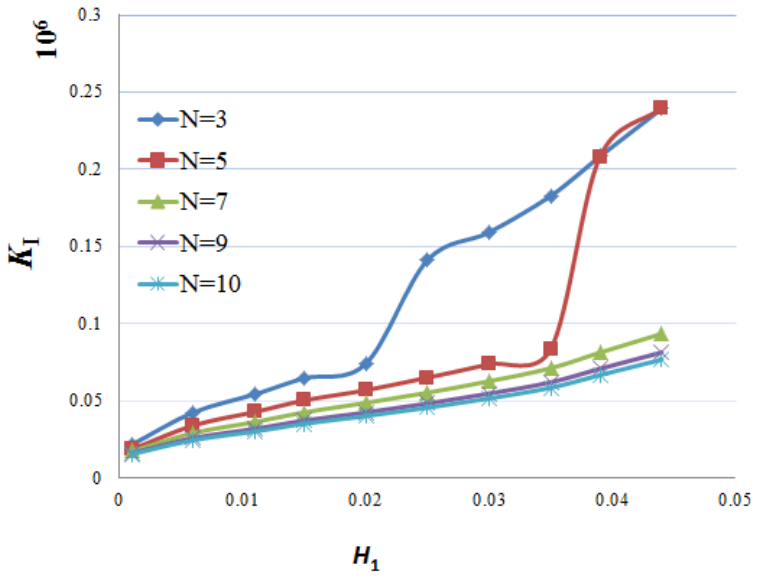

Figure 9. 1 Progress of the K_I [10^6·Pa·$m^{1/2}$] function dependent on the initial crack length H_1 for all variant of used number of layers N with H_2 = 0.5 (J. Sobek, et al.,2017)

A second analysis was done for the same values of the parameter N, but in this case the value of H_2 is 0.8 (this means that the solid part is 80 % of the test specimen width). In the Figure 9.2 we can appreciate the same trend of accuracy as in the previous case. Again, the accuracy of the low number of layers used is balanced with N = 7. As in the previous case, optimal number of layers is N = 10 and more (J. Sobek, et al.,2017).

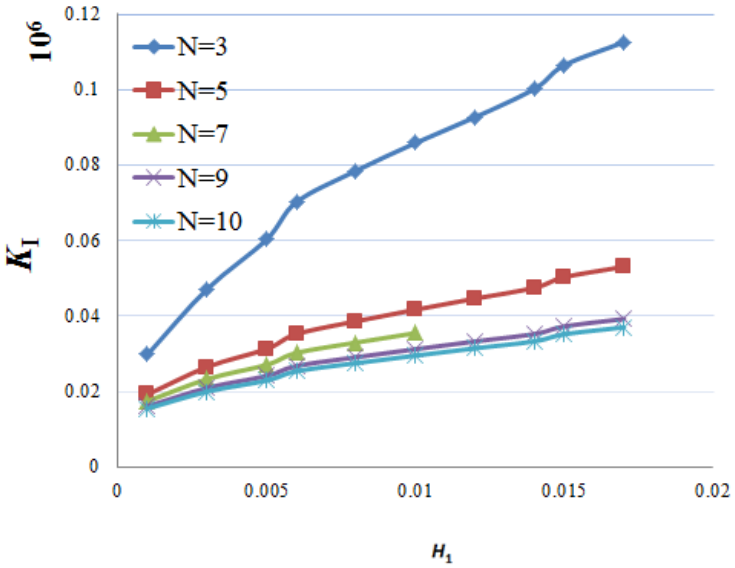

Figure 9. 2 Progress of the K_I [10^6·Pa·$m^{1/2}$] function dependent on the initial crack length H_1 for all variant of used number of layers N with H_2 = 0.8 (J. Sobek, et al.,2017)

9.2 INFLUENCE OF THE ANGLE CHANGING OF CHEVRON NOTCH

A second analysis is based on changing of the value of the chevron notch angle. We used the parameter α_0 (initial crack length, relative value) to characterize this angle. The changes on this parameter are done to see the influence of it on the value of the stress intensity factor (K_I). For all the results obtained it was used the value of B_N = 0.003 m. For each value of α_0 the graphs are shown from Figure 9.3 to Figure 9.11. There is also a last graph in which a comparison is done for all values of the K_I for the different values of α_0.

The first angle studied is for α_0 = 0.0. For this value, we have the results expressed in the correspondent graph below Figure 8.3. In this graph, we can see that the critical value for which the K_I starts to change is small, the value of the stress intensity factor seems to be more stable for lower values of α_1 with tendency to the value of K_I = 1000 Pa$\sqrt{m}$.

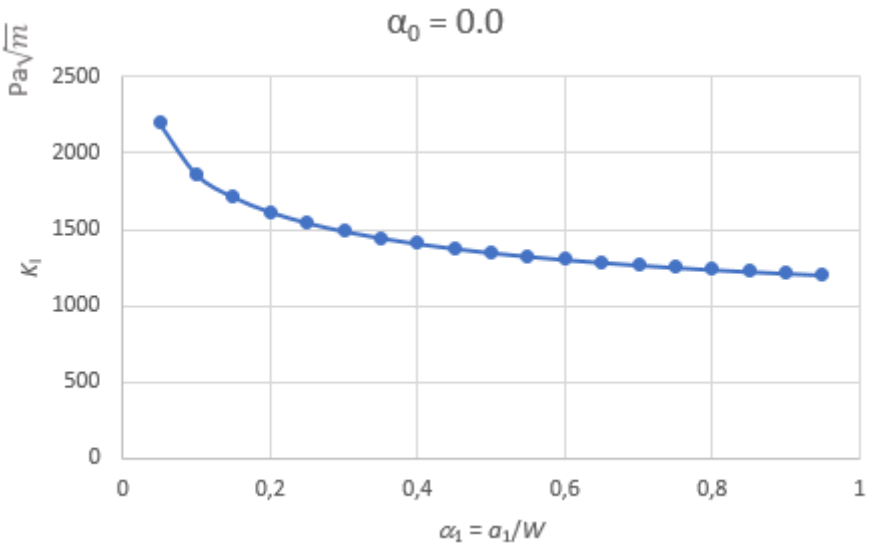

Figure 9. 3 Stress intensity factor vs α_1 for parameter α_0 = 0.0

For the value of α_0 = 0.1, the correspondent graph is shown below in Figure 9.4. In this graph, we can see that like the previous case there are not much values in which the K_I is stable, there is a peak for α_1 approximately 0.1 and from that point the K_I tends to decrease.

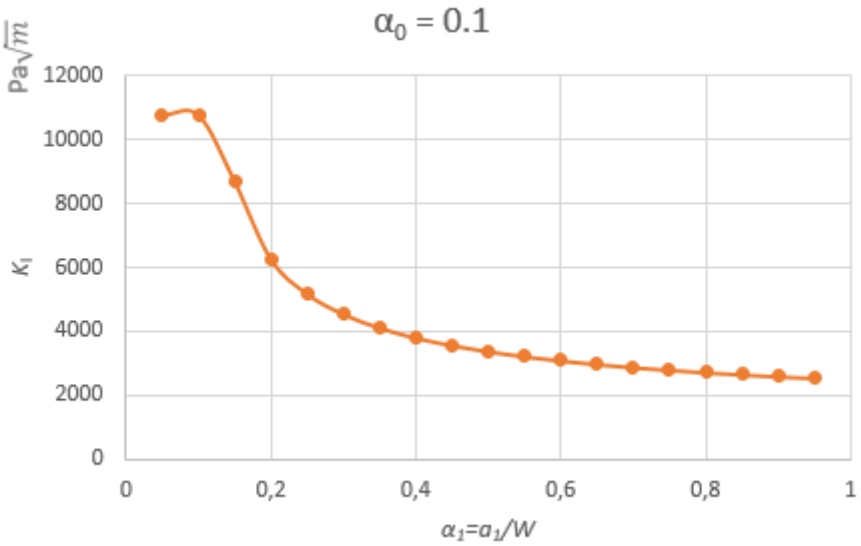

Figure 9. 4 Stress intensity factor vs α_1 for parameter α_0 = 0.1

The next graph represented is for the value of $\alpha_0 = 0.2$. In this case, we can appreciate a little more of stability than in the previous ones. The value of the peak is for $\alpha_1 = 0.2$

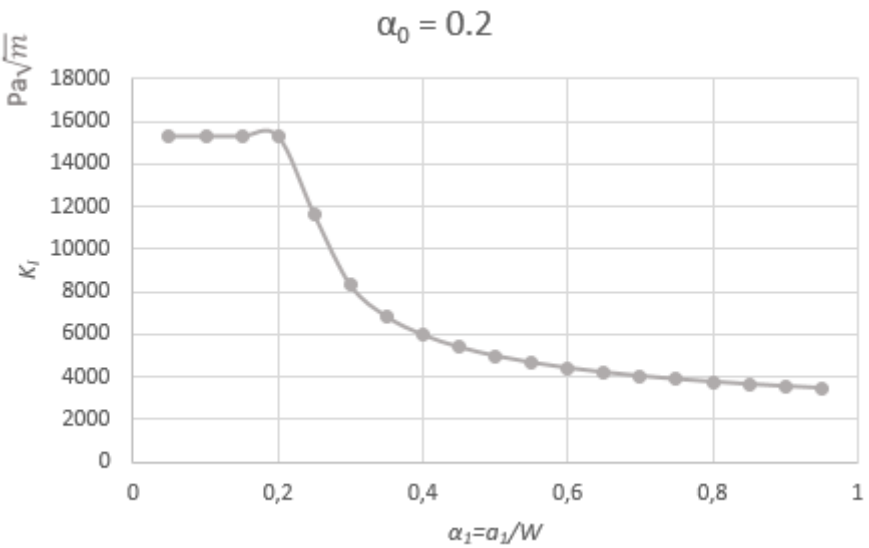

Figure 9. 5 Stress intensity factor vs α_1 for parameter $\alpha_0 = 0.2$

For the value of $\alpha_0 = 0.3$ that is shown in Figure 9.6 the K_I is stable and with value 20000 Pa$\sqrt{m}$ until α_1 is equal to 0.3.

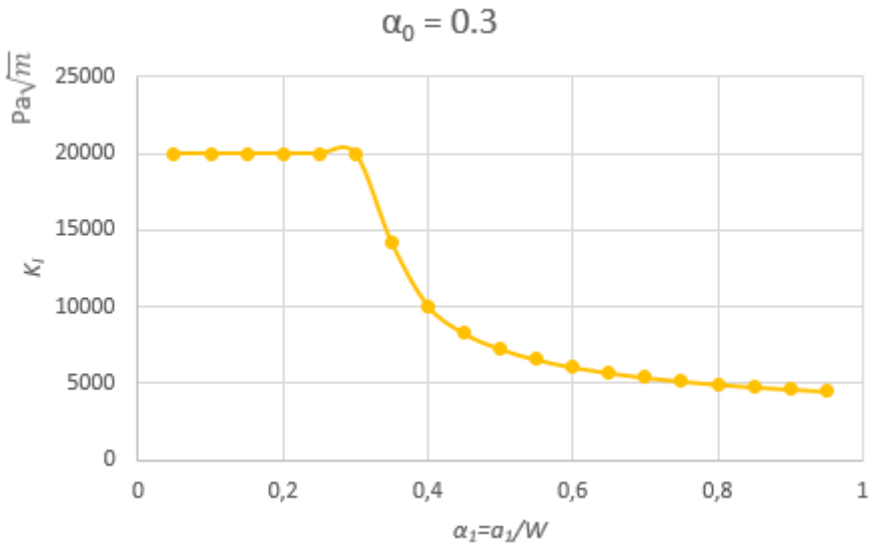

Figure 9. 6 Stress intensity factor vs α_1 for parameter $\alpha_0 = 0.3$

In Figure 9.7 we can appreciate the results obtained for $\alpha_0 = 0.4$

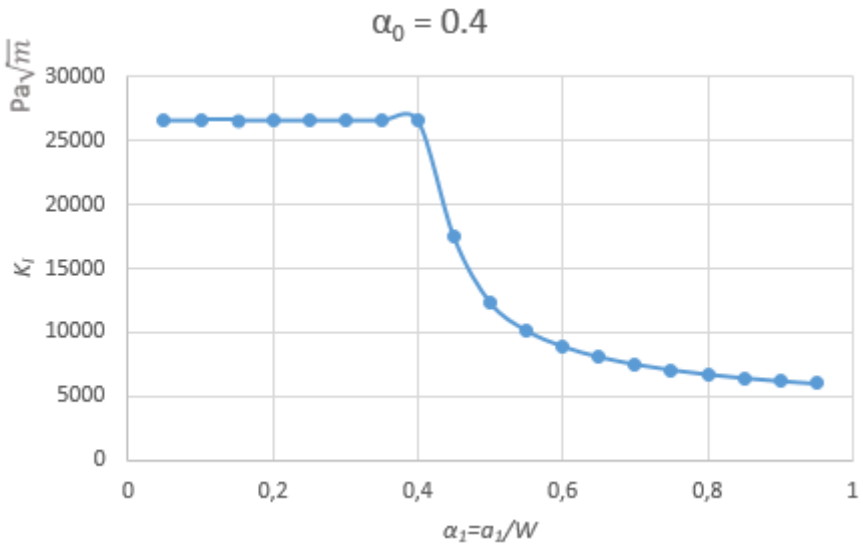

Figure 9. 7 Stress intensity factor vs α_1 for parameter $\alpha_0 = 0.4$

In figure 9.8 we can appreciate the results obtained for $\alpha_0 = 0.5$

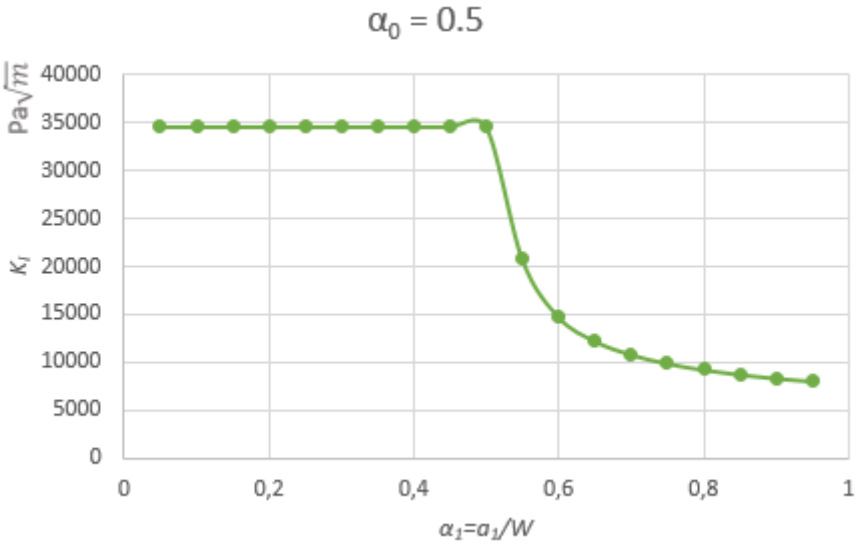

Figure 9. 8 Stress intensity factor vs α_1 for parameter $\alpha_0 = 0.5$

In Figure 9.9 we can appreciate the results obtained for $\alpha_0 = 0.6$

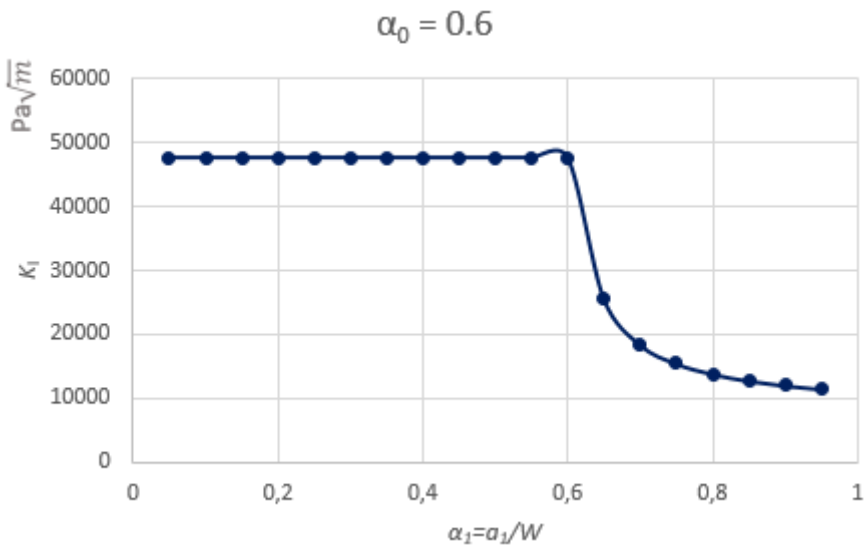

Figure 8. 9 Stress intensity factor vs α_1 for parameter $\alpha_0 = 0.6$

In Figure 9.10 we can appreciate the results obtained for $\alpha_0 = 0.7$

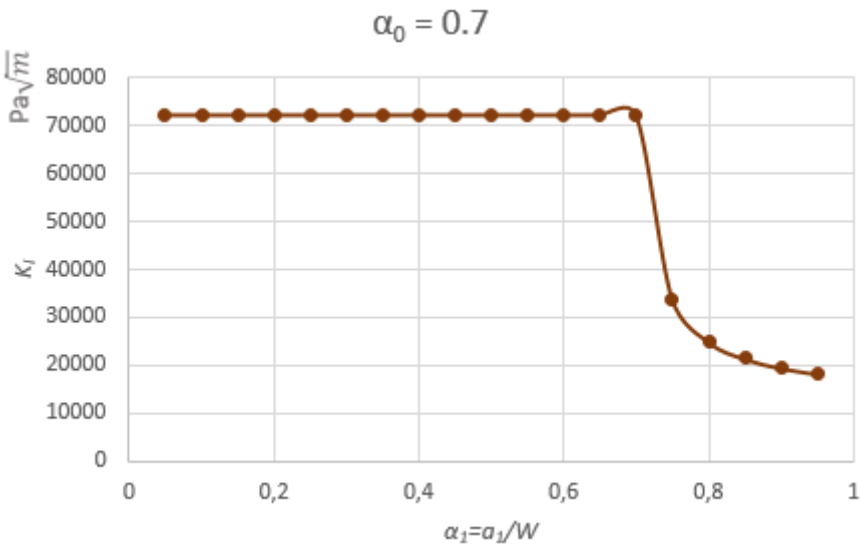

Figure 9. 10 Stress intensity factor vs α_1 for parameter $\alpha_0 = 0.7$

In Figure 9.11 we can appreciate all the graphs above joined together in the same chart so we can compare the values obtained in all of them.

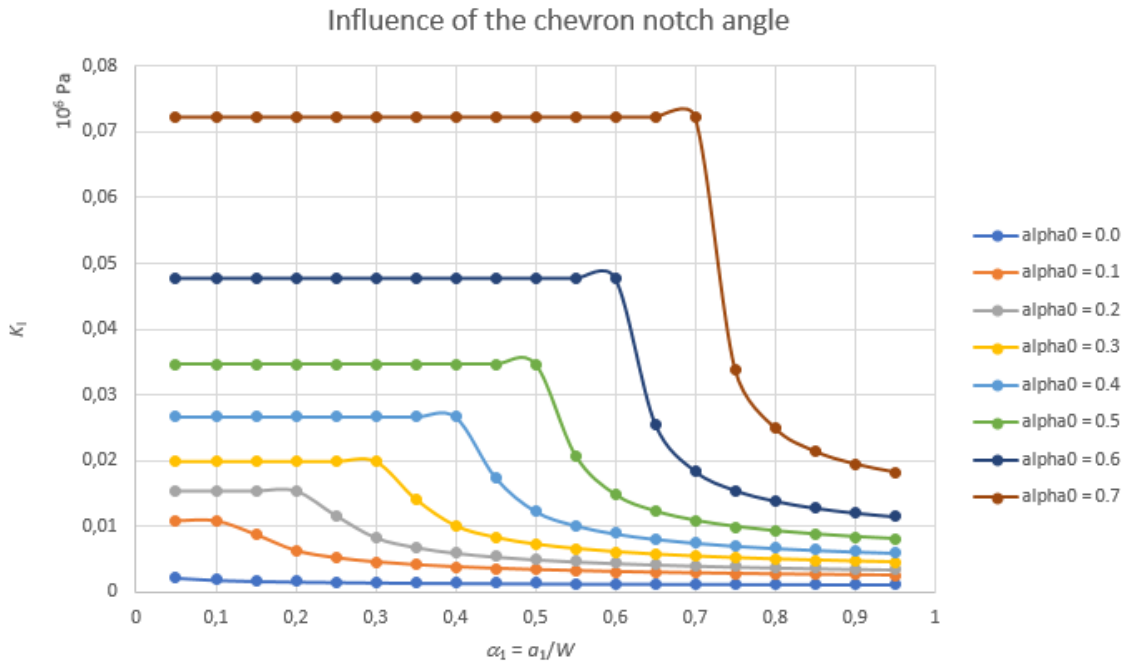

Figure 9. 11 Influence of the chevron notch angle on the stress intensity factor [Pa·m$^{1/2}$] for a 4PB test specimen

9.3 INFLUENCE OF THE THICKNESS OF CHEVRON NOTCH PART IN THE CENTER OF THE TEST SPECIMEN

In this last analysis, the parameter that is going to be changed to see the effect that it has on the stress intensity factor (K_I), is the B_N (thickness of the chevron notch). This analysis is going to be structured in two parts, the first one is going to be for different values of α_0 (constant value in each case) what happens with the K_I for different values of α_1, depending on the B_N. This study can be seen in Figures from 9.12 to 9.14. The second part is going to be the opposite way, it means that for some values of α_1 that remain constant we are going to see what happens with K_I for different values of α_0, again depending on the thickness of the chevron notch B_N. This second part can be seen in Figure 9.15 to Figure 9.17.

In the figure below the influence of the chevron notch thickness is represented for a constant value of α_0 (in this case 0.0) and changeable values of α_1. We can see that the values do not vary too much for the different values of α_1 and also, another thing to take into account is that from B_N = 0.004 m the changes on the value of K_I are really small for all values of α_1.

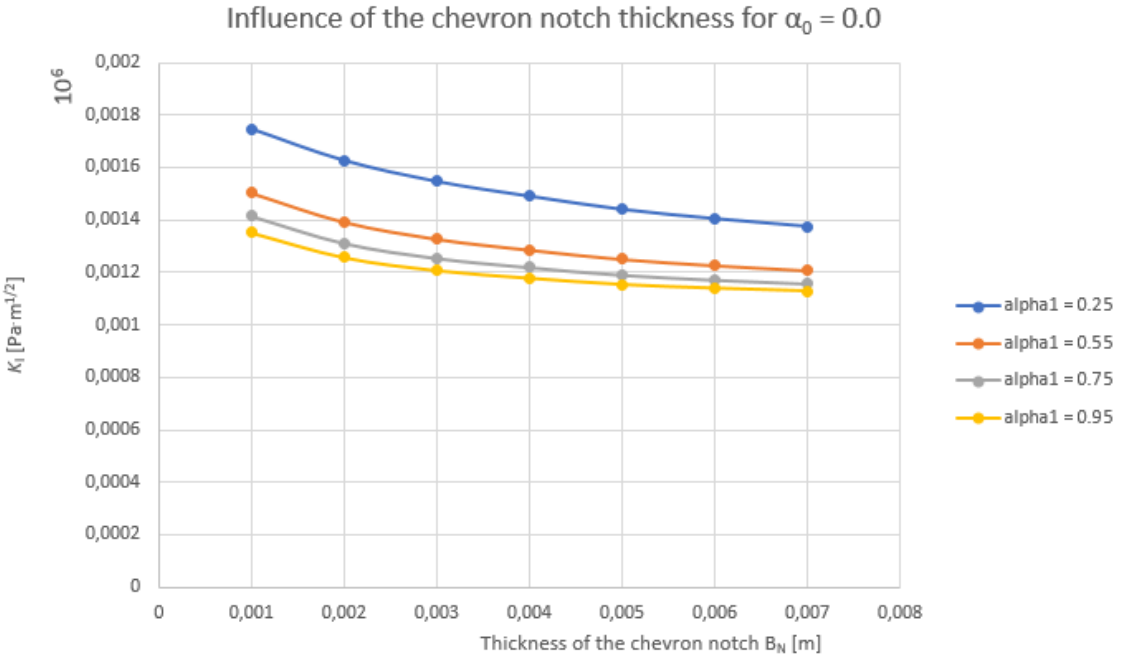

Figure 9. 12 Influence of the chevron notch thickness for different values of α_1 and α_0 = 0.0

In the Figure 9.13 the influence of the chevron notch thickness is represented for a constant value of α_0 (in this case 0.2) and changeable values of α_1. We can see that the only value of α_1 in which we can appreciate some difference in the results obtained is 0.25, the rest of the values behave in the same way as in the previous case (now the values are smaller but the behaviour remains almost the same, no big variations on the value of K_I for the different B_N values).

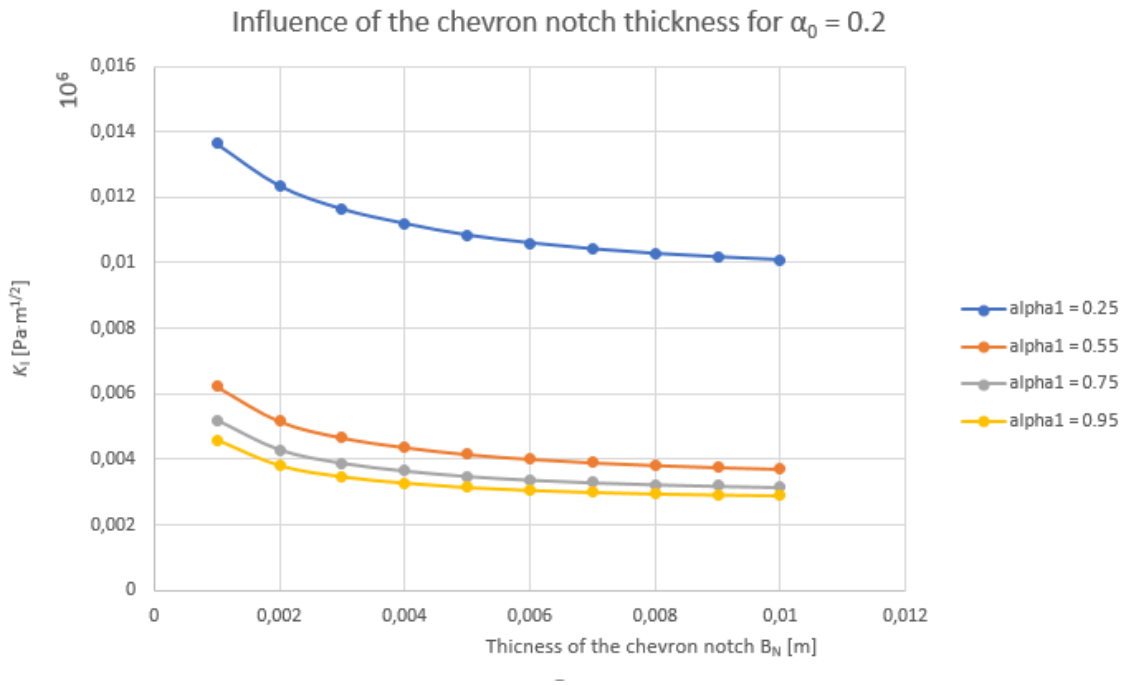

Figure 9. 13 Influence of the chevron notch thickness for different values of α_1 and α_0 = 0.2

In the Figure 9.14 the influence of the chevron notch thickness is represented for a constant value of α_0 (in this case 0.5) and changeable values of α_1. We can appreciate that in this case all the values of K_I are much smaller than in the two previous cases (in this case the higher value is less than K_I = 0.02 Pa$\sqrt{m}$).

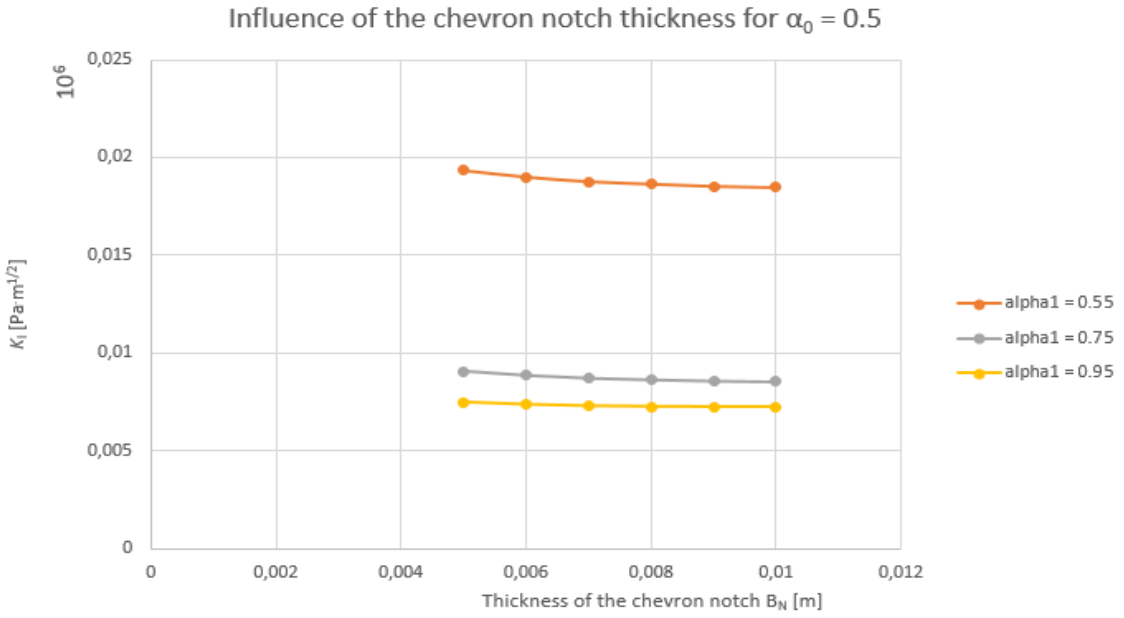

Figure 9. 14 Influence of the chevron notch thickness for different values of α_1 and α_0 = 0.5

In the Figure 9.15 the influence of the chevron notch thickness is represented for a constant value of α_1 (in this case 0.55) and changeable values of α_0. We can see that for the values of α_0 0.2 and 0.0 the results are not so different, but for the value of $\alpha_0 = 0.5$ the K_I is higher. In all the cases with independence on the value of α_0 the K_I experiments a really small variation for the different B_N.

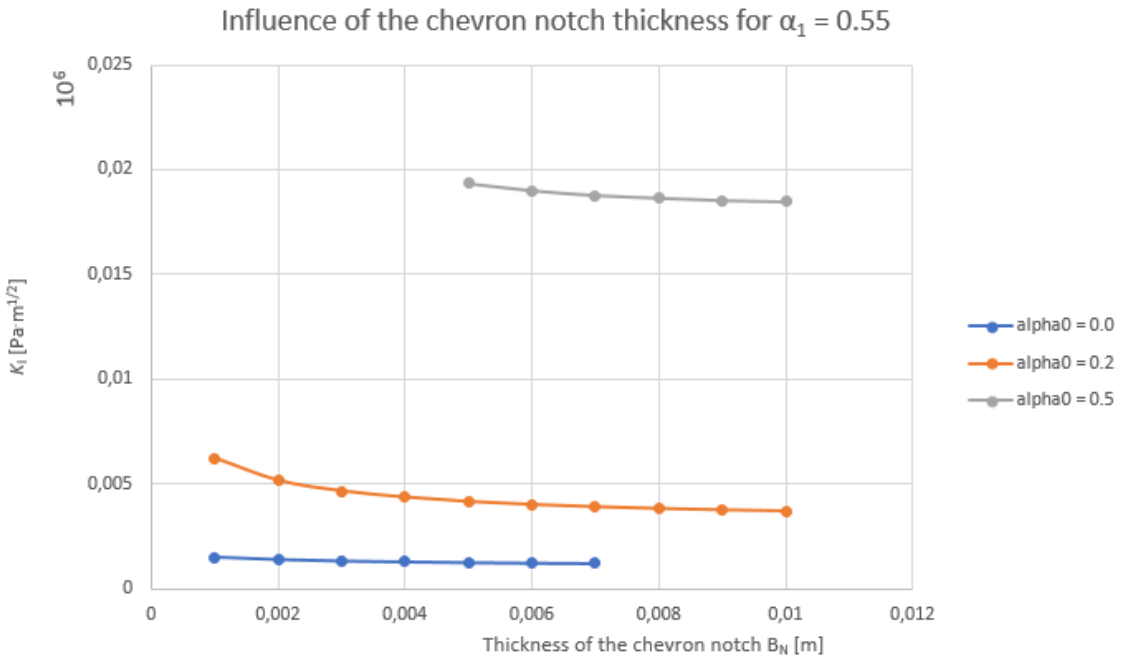

Figure 9. 15 Influence of the chevron notch thickness for different values of α_0 and $\alpha_1 = 0.55$

In the Figure 8.16 the influence of the chevron notch thickness is represented for a constant value of α_1 (in this case 0.75) and changeable values of α_0. The behaviour is practically the same as in the previous case, the values are smaller in this case but the tendency is the same.

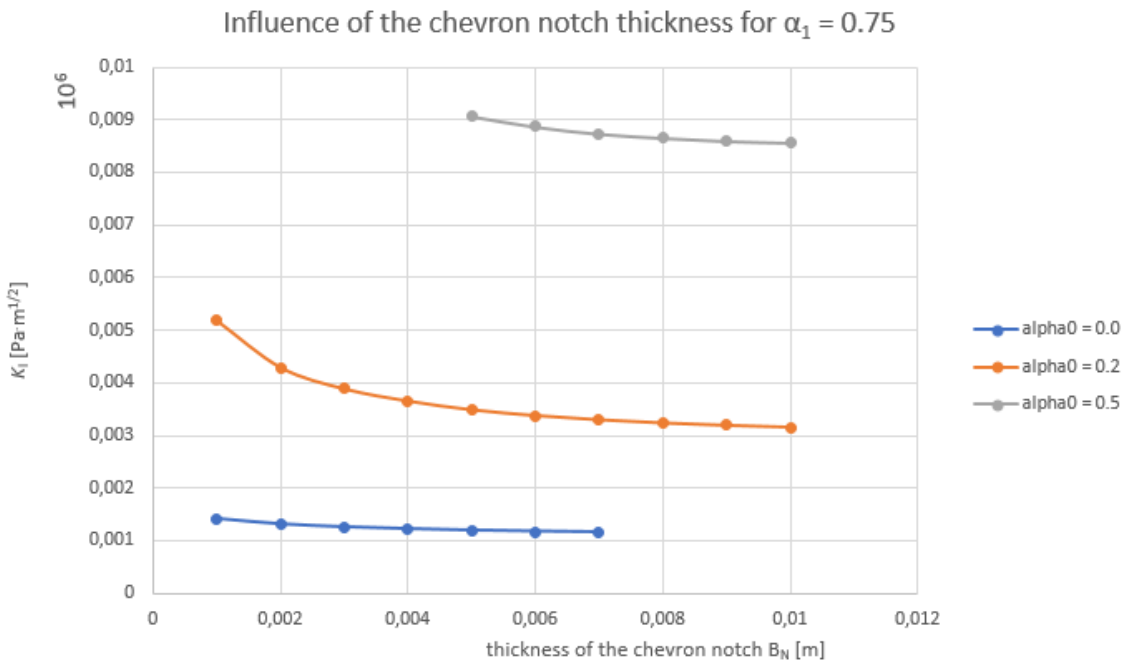

Figure 9. 16 Influence of the chevron notch thickness for different values of α_0 and $\alpha_1 = 0.75$

In the Figure 9.17 the influence of the chevron notch thickness is represented for a constant value of α_1 (in this case 0.95) and changeable values of α_0.

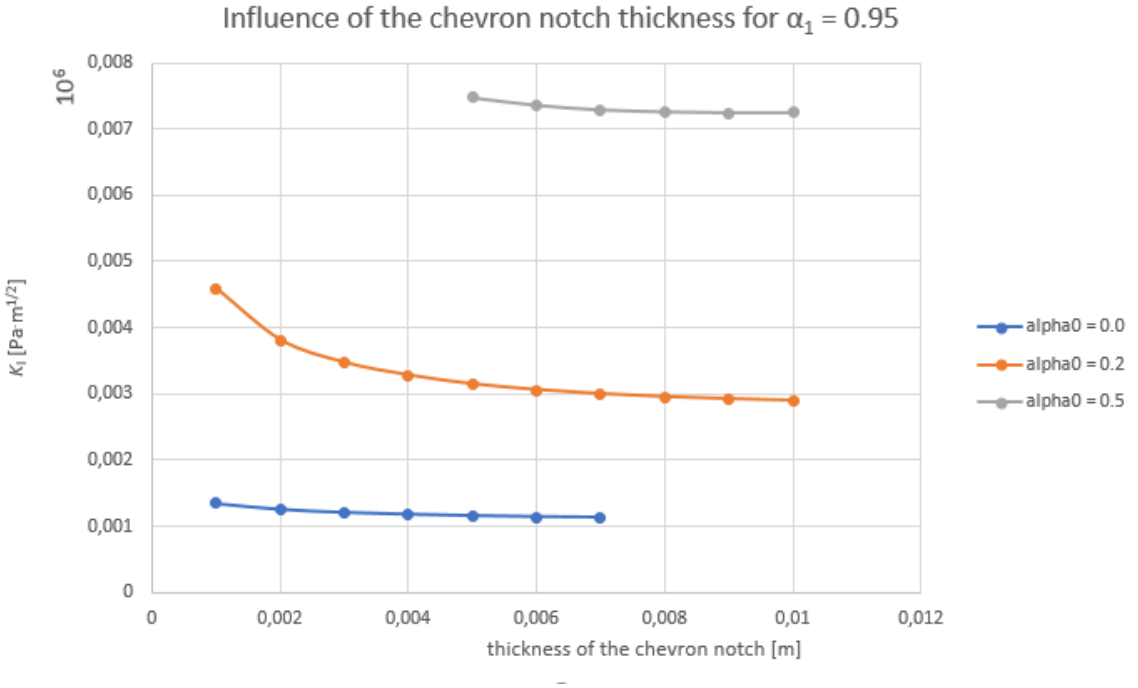

Figure 9. 17 Influence of the chevron notch thickness for different values of α_0 and $\alpha_1 = 0.95$

10. Conclusion

10.1 IMPACT OF THE NUMBER OF LAYER USED

Successful implementation of the initial chevron notch into the numerical models of the test specimens subjected to the 3PB configuration was performed for the plane stress problem. Recommendation is to solve the numerical model with at least 7 layers – optimal number is 10 layers (N = 10) and more.

The model is prepared for the further parametric analysis – with the changes of many other variables, like an initial crack length, an angle of the chevron notch, span, width of the solid part of the cross-section, etc.

10.2 INFLUENCE OF THE ANGLE CHANGING OF CHEVRON NOTCH

For the study done with the 4PB geometry, it can be appreciated in the previous graphs (look at Figure 9.3 to Figure 9.11) that the value of the stress intensity factor is more stable for higher values of the chevron notch angle. When this angle is increased the value of α_1 for which the stress intensity factor changes abruptly, is higher. We can also appreciate that the stability of K_I is in all cases maintained until the value of α_1 is equal to the value of α_0.

10.3 INFLUENCE OF THE THICKNESS OF CHEVRON NOTCH PART IN THE CENTER OF THE TEST SPECIMEN

For the first part of the analysis, in the Figures from 9.12 to 9.14, it can be appreciated that as we increase the value of α_0, the effect of the B_N is higher, it means that for higher values of α_0 the influence of the thickness of the chevron notch is more important.

For the second part of the analysis, in the Figures from 9.15 to 9.17, we can see that for small values of B_N the only value of α_0 that may affect more to the value of K_I is α_0 = 0.2. Also, as we increase the value of α_1 for the same B_N and the same α_0 the value of K_I is lower.

11. Nomenclature

11.1 LIST OF SYMBOLS

A_n → Coefficients of the terms of the Williams series, constants for a value of the crack length

A → Crack length [mm]

a_1 → Parameter which characterizes the ending of the linear function of the chevron notch, measured from the bottom part of the test specimen [m]

B → Thickness of the specimen [m]

B_N → Thickness of chevron notch [m]

B_P → Thickness of the steel part [m]

E → Young modulus [Pa]

F → Force applied into the test specimen [N]

H_1 → Initial crack length, absolute value [m]

H_2 → Distance from the end of the specimen to the beginning of the crack [m]

H_P → Thickness of the steel part [m]

K → Stress intensity factor [Pa$\sqrt{m}$]

k→ Kolosov´s constant

K_C → Fracture toughness [Pa$\sqrt{m}$]

K_I → Stress intensity factor corresponding to the mode I of loading [Pa$\sqrt{m}$]

K_{II} → Stress intensity factor corresponding to the mode II of loading [Pa$\sqrt{m}$]

K_{III} → Stress intensity factor corresponding to the mode III of loading [MPa$\sqrt{m}$]

L → Length of the specimen [m]

N → Number of layers used

P → Pick force taken from loading diagram [N]

S → Span of supports [m]

W → Width of the specimen [m]

X, Y, Z → Cartesian coordinate system

α_0 = alpha0→ initial crack length, relative value

α_1 → division of a_1/W

r, ϑ → Polar coordinate system

v → Poisson coefficient

μ → Shear modulus [Pa]

{σ} → Stress tensor

{u} → Displacement vector

11.2 LIST OF ABBREVIATIONS

ASTM → American Society for Testing and Materials

EPFM → Elastic Plastic Fracture Mechanics

FE → Finite Element

LEFM → Linear Elastic Fracture Mechanics

3PB test → Three-point bending test

4PB test → Four-point bending test

12. References

A.R. BOCCACCINI, R.D. RAWLINGS, I. DLOUHÝ. Materials science and engineering. Volume 347. Pp 102-108 (25 April 2003)

ANDERSON, Ph.D. Fracture Mechanics. Fundamentals and applications. Third edition CRC-Press (2005)

BARENBLATT, G. I. The formation of equilibrium cracks during brittle fracture: General ideas and hypotheses, axially symmetric cracks. Journal of Applied Mathematics and Mechanics, 23. 1959, pp. 622–636.

BAŽANT, Z. P. Size effect in blunt fracture: concrete, rock, metal. Journal of Engineering Mechanics ASCE, 110 (4). 1984, pp. 518–535.

DEFINITION OF ANSYS. http://www.ansys.com/

DIETRICH G. MUNZ, JOHN L. SHANNON, JR., AND RAYMOND T. BUBSEY. Fracture toughness calculation from maximum load in four-point bend tests of chevron notch specimens. (1980)

D. MUNZ, R.T. BUBSEY and J.E. SRAWLEY. Compliance and stress intensity coefficients for short bar specimens with chevron notches. International Journal of Fracture, Vol 16, No. 4, (August 1980)

DUGDALE, D. S. Yielding of steel sheets containing slits. Journal of Mechanics and Physics of Solids, 8 (2). 1960, pp. 100–104.

FISCHER CRIPPS, Introduction to Contact Mechanics. XXII, 226 p. hardcover- 2007

FOUR POINT BENDING TEST IMAGE. http:// www.substech.com

FOUR POINT BENDING TEST. https:// www.researchgate.net

FRANCISCO JAVIER BELZUNCE VARELA, book of notes subject Technology Of Materials used in Universidad de Oviedo (Escuela Politécnica de Ingeniería)- 2014

GRIFFITH, A. A. The phenomena of rupture and flow in solids. Philosophical Transaction Of the Royal Society, London. 1921, pp. 163–198.

H.G. TATTERSALL AND G. TAPPIN, Journal of Materials Science, 1 (1966) 296--301.

HILLERBORG, A., MODÉER, M., PETERSSON, P. E. Analysis of crack formation and crack growth in concrete by means of fracture mechanics and finite elements. Cement and concrete research, 6. 1976, pp. 773–782.

IRWIN, G. R. Analysis of stresses and strains near the end of a crack traversing a plate. Journal of Applied Mechanics, Transaction of the ASME, 24. 1957, pp. 361–364.

IRWIN, G. R. Crack extension force for a part-through crack in a plate. ASTM Bullet, 243. 1960, pp. 29–40.

INITIAL CHEVRON NOTCH. http://www.lmc.ep.usp.br/people/umberto/research/sr1-i.html

J. C. NEWMAN J JR. NASA Langley Research Center Hampton, Virginia. A review of chevron-notched fracture specimens. (September 1984)

JENQ, Y. S., SHAH, S. P. A two-parameter fracture model for concrete. Journal of Engineering Mechanics, 111(4). 1985, pp. 1227–1241.

J. BLUHM. Engineering Fracture Mechanics 7 (1975). 593-604

J. NAKAJAMA, Journal of the American Ceramic Society, 48 (1965) 583-587.

J. SOBEK, S. GONZÁLEZ MENÉNDEZ AND S. SEITL. Numerical modelling of a chevron notched bend specimen – plane model. (2017)

L. M. BARKER, in Fracture Mechanics Applied to Brittle Materials, STP 678, American Society for Testing and Materials, Philadelphia (1979) 73-82.

M. G. JENKINS, A. S. KOBAYASHI, K. W. WHITE and R. C. BRADT. Department of MechanicalEngineering,2Department of Materials Science and Engineering, College of Engineering, University of Washington, Seattle, WA 98195, USA. International Journal of Fracture 34:281-295 (1987)

MUSKHELISHVILI, N. I. Some Basic Problems in the Theory of Elasticity. Noord hoof, Netherlands. First edition in English 1953. Original in Russian 1933.

POOK, L.P. An Approach to quality control K_{IC} Test piece, International Journal of Fracture Mechanics, Vol 8, pp.103-108 (1972)

REINHARDT, H. W., XU, S. Crack extension resistance based on the cohesive force in concrete. Engineering Fracture Mechanic, 64. 1999, pp. 563–587.

RICE, J. R. A path independent integral and the approximate analysis of strain concentration by notches and cracks. Journal of Applied Mechanics ASME, 35: 1968, pp. 379–386.

R.W. DAVIDGE AND G. TAPPIN, in Proceedings of the British Ceramic Society 15 (1970) 47-60

SHAILENDRA KUMAR AND UDHIRKUMAR V. BARAI. Concrete Fracture Models and Applications. Springer Heidelberg Dordrecht London New York. 2011

V. VESELÝ, P. FRANTÍK, J. SOBEK, L. MALÍKOVÁ and S. SEITL. Multi-parameter crack tip stress state description for evaluation of nonlinear zone width in silicate composite specimens in component splitting/bending test geometry. Received Date: 6 October 2013; Accepted Date: 24 January 2014; Published Online: 2014

WILLIAMS, M. L., ELLINGER, G. A. Investigation of Structural Failures of Welded Ships. The Welding Journal, Vol. 32 (10). 1953, pp. 498–528.

WILLIAMS, M. L. On the stress distribution at the base of a stationary crack. ASME Journal of Applied Mechanics, 24. 1957, pp. 109–114.

WESTERGAARD, H. M. Bearing Pressures and Cracks. Journal of Applied Mechanics, Vol. 6. 1939, pp. 49–53.

WU, SHANG-XIAN. An Investigation of Chevron-Notch Three-Point Bend Fracture Toughness Specimen, International Journal of Fracture, Vol. 19, 1982, pp. R27-R30.

13. CV

Name: Sofía González Menéndez

E-mail: sofiagonzalezmenendez@gmail.com

Date of birth: 21 August 1991

Education:

- Universidad de Oviedo, Asturias (Spain)
  2009-2014, Industrial Engineering (Bachelor)
- Santa María del Naranco, Oviedo (Spain)
  2007-2009 Technical studies
- Additional Information on Education
  Now studying Master in Industrial Engineering. First year in the same university as the bachelor (Universidad de Oviedo). Second year to be finished in May 2017 in Czech Republic—Brno University of Technology, Faculty of Civil Engineering

Courses and training:

- Cornell University (online course)
  06-2016/07-2016. A hands-on Introduction to Engineering Simulations
- Dartmouth (online course)
  08-2016/09-2016. The engineering of Structures around us

Employment History:

- Banco Sabadell (Spain)
  06-2014/08-2014. Internship focused on client service and supporting the rest of the team when needed.

14. Appendix

14.1 CODE FOR 3PB TEST

```
/UIS, MSGPOP, 3

/UIS, Label, VALUE      ! NO WARNINGS



FINISH

/CLEAR, NOSTART


*CFOPEN, KCALTXT, TXT                    ! OPEN THE TEXT FILE


W=0.1

*DO, N,3,9,2! AUTOMATIC LOOP FOR N

*DO, ALPHA,0.5,0.9,0.1 ! ALPHA LOOP


H2=(ALPHA*W)

H1LENGTHTOH2=(W-H2-0.002)/10

*DO, H1,0.001, (W-H2-0.002), H1LENGTHTOH2! H1 LOOP


! START***************

! MODEL CHEVRON, TWO SUPPORTS, SUPPORT ALONG 4MM
```

```
/PREP7


! PARAMETERS********

L=0.4

S=0.36     ! S/L=0.9

DILEK1=0.0001  ! SIZE OF ELEMENTS

ELSICRACK=0.0001! SIZE OF ELEMENTS AT THE CRACK TIP

ROZETA=3         ! SIZE OF ELEMENTS KSCON

FORCE=1000                ! FORCE VALUE IN N

B=0.1

! H1=0.0001! NEEDS TO BE STARTED FROM NON-ZERO VALUE TO CONNECT THE GEOMETRY

! W=0.1 ! COMMAND LINE HAS BEEN CHANGED

! H2=(ALPHA*W)

BN=0.003

HP=0.001

! N=10! NUMBER OF LAYERS

LAY=(W-H1)/N! LAYER THICKNESS

! ALPHA=(W-H1)/W




! DEFINITION OF ET, MAT, REAL********

ET,1, PLANE82,,,3

MP, EX,1,35E9

MP, PRXY,1,0.2

MP, EX, 333,100        ! MATERIAL FOR ZERO LAYER
```

```
MP, PRXY,333,0.2      ! MATERIAL FOR ZERO LAYER

R,1,0.000000000000001   ! WE HAVE TO CHOOSE A VALUE APROXIMETELY 0 BUT NOT 0

*IF, H2, EQ,0, THEN
        *DO, RLOOP,2, N+1,1                    !CREATION OF REAL CHARACTERISTICS
        THICKNESSOFLAYER=(B*LAY*(RLOOP-1))/(W-H1-H2)
        R, RLOOP,THICKNESSOFLAYER              !THICKNESS
        *ENDDO

*ELSE
        *DO, RLOOP, 2, N+1,1                   !CREATION OF REAL CHARACTERISTICS
        H3=(RLOOP-1) *LAY
        *IF, H3, LT, (W-H1-H2), THEN
                THICKNESSOFLAYER=(B*LAY*(RLOOP-1))/(W-H1-H2)
                R, RLOOP, THICKNESSOFLAYER      ! THICKNESS

        *ELSE
        R, RLOOP,B                      !THICKNESS
        *ENDIF
        *ENDDO
*ENDIF

! DEFINITION ET, MAT, REAL STEEL********
```

```
ET,222, PLANE82,,,3

MP, EX,222,210E9

MP, PRXY,222,0.3

R,222, B



!ENTER OF KP********

K,1,0,0                    !CRACK TIP

K,2, H1

K,3, -(W-H1)

K,4, ,(BN/2)

K,5, H1, (BN/2)

K,6, H1, (L/2)

K,7, -(W-H1), (L/2)

K,8, -(W-H1), (BN/2)

K,9, -(W-H1+HP), (BN/2)

K,10, -(W-H1+HP)


*DO, KCR,1,N-1,1     !STRING FOR THE CREATION OF THE NODES

   K,,-KCR*LAY

   K,,-KCR*LAY,(BN/2)

*ENDDO



!AREAS********

L,5,6        !L1
```

```
L,6,7        !L2

L,7,8        !L3


A,3,8,9,10    !A1 STEEL


A,1,2,5,4                          !A2

A,1,4,12,11        !A3


*DO,ACR,1,N-2,1       !AREAS FROM 4 TO 4+(N-3)

   A,11+(ACR-1)*2,10+(ACR)*2,14+(ACR-1)*2,13+(ACR-1)*2

*ENDDO


A,(10+(N-1)*2)-1,10+(N-1)*2,8,3                    !AREA 4+(N-2)


FLST,2,(5+N-1),4

FITEM,2,1

FITEM,2,2

FITEM,2,3

FITEM,2,10

FITEM,2,12

*DO,ACR2,1,N-1,1

FITEM,2,(12+3*ACR2)

*ENDDO

AL,P51X


ALLSEL
```

```
!SIZE OF AREAS********

AESIZE,ALL,0.001,

!CREATION OF KSCON********

KSCON,4,ELSICRACK,1,ROZETA,0.75


!MESH CONCRETE

TYPE,1

MAT,1


*DO,AMESHLOOP,2,N+1,1    !MESHING OF AREAS

   REAL,AMESHLOOP

   AMESH,AMESHLOOP+1

*ENDDO


!MESH STEEL

AESIZE,ALL,0.001,

TYPE,222

MAT,222

REAL,222

AMESH,1


!MESH CONCRETE (ZERO THICKNESS)

TYPE,1

MAT,333
```

```
REAL,1

AMESH,2


AESIZE,ALL,0.005,   !MESHING OF THE BIGGEST AREA

R,(N+3),B              ! THE BIGGEST AREA

MAT,1

REAL,(N+3)

AMESH,(N+3)



!BOUNDARY CONDITIONS********

ALLSEL

LSEL,S,LOC,Y,0

LSEL,U,LINE,,7,8

NSLL,S,1

D,ALL,UY

ALLSEL


NSEL,S,LOC,X,H1

NSEL,R,LOC,Y,(S/2)-0.002,(S/2)+0.002

D,ALL,UX

ALLSEL


KSEL,S,KP,,10,10

NSLK

F,ALL,FX,FORCE
```

```
ALLSEL

EPLO
/SHRINK,0
/ESHAPE,1
/EFACET,1
/RATIO,1,1,1
/CFORMAT,32,0
/REPLOT



!CALCULATION**************************
/SOLU
SOLVE



!RESULTS*************************
/POST1
SET,FIRST

KSEL,S,KP,,4,4
NSLK
*GET, NCRACKTIP, NODE, 0, NUM, MIN
ALLSEL
```

```
NSEL,S,LOC,Y,(BN/2)          !NODE SELECTION IN THE WAY OF LOADING
NSEL,R,LOC,X,ELSICRACK,0
NSEL,U,NODE,,NCRACKTIP

*GET, NUMBEROFNODES, NODE, 0, COUNT

    *IF,NUMBEROFNODES,EQ,2,THEN
    *GET, NMINKCALC, NODE, 0, NUM, MIN
    *GET, NMAXKCALC, NODE, 0, NUM, MAX
    NSEL,A,NODE,,NCRACKTIP
    LPATH,NCRACKTIP,NMAXKCALC,NMINKCALC  !NODES SELECTED
    KCALC,1,1,0,1

    *GET,KI1,KCALC,0,K,1              !MUST BE CHECKED

    *VWRITE,N,ALPHA,H1,H2,KI1
(F5.0,'   ',F5.3,'   ',F5.3,'   ',F5.3,'   ',F20.10)
!(F5.3,'               ',F20.10)
ALLSEL

    *ENDIF

/PREP7
ALLSEL
ACLEAR,ALL
```

```
ADEL,ALL

LDEL,ALL

KDEL,ALL


*ENDDO      !END H1 LOOP

*ENDDO      !END ALPHA LOOP

*ENDDO      !END N LOOP


!FINISH

!/CLEAR,NOSTART


*CFCLOSE                !CLOSES TEXT DOCUMENT
```

14.2 CODE FOR 4PB TEST

```
/UIS, MSGPOP, 3

/UIS, Label, VALUE        !NO WARNINGS



FINISH

/CLEAR,NOSTART


*CFOPEN,KCALTXT,TXT             !OPEN THE TEXT FILE


W=0.1

ALPHA=0       !0,0.2,0.5

H1=(ALPHA*W)+0.0005        !FOR THE REST (THEN THE 0 VALUE)) DELETE THE +0.0005

*DO,H2START,0.05,0.95,0.05   !H2 LOOP,0.25-0.95,0.5-0.95

ALENGTH=W*H2START

H2=W-ALENGTH

!H2=W-H1-(H2START*W)           !DIFFERENT WAY

!START***************

!MODEL CHEVRON, 4PB, TWO SUPPORTS, SUPPORT ALONG 4MM



/PREP7
```

```
!PARAMETERS********

L=0.825

S=0.8       !S/W=0.8

DILEK1=0.0002  !SIZE OF ELEMENTS

ELSICRACK=0.0002  !SIZE OF ELEMENTS AT THE CRACK TIP

ROZETA=3         !SIZE OF ELEMENTS KSCON

FORCE=100                  !FORCE VALUE IN N

B=0.1

BN=0.003

BP=0.003

HP=0.001

N=30    !NUMBER OF LAYERS

LAY=(W-H1)/N    ! LAYER THICKNESS



!DEFINITION OF ET, MAT, REAL********

ET,1,PLANE82,,,3

MP,EX,1,72.39482E9

MP,PRXY,1,0.3

MP,EX,333,100         !MATERIAL FOR ZERO LAYER

MP,PRXY,333,0.2       !MATERIAL FOR ZERO LAYER


R,1,0.000000000000001   ! WE HAVE TO CHOOSE A VALUE APROXIMETELY 0 BUT NOT 0


*IF,H2,EQ,0,THEN

        *DO,RLOOP,2,N+1,1                    !CREATION OF REAL CHARACTERISTICS
```

```
        THICKNESSOFLAYER=(B*LAY*(RLOOP-1))/(W-H1-H2)
        R,RLOOP,THICKNESSOFLAYER            !THICKNESS
        *ENDDO

*ELSE
        *DO,RLOOP,2,N+1,1                   !CREATION OF REAL CHARACTERISTICS
        H3=(RLOOP-1)*LAY
        *IF,H3,LT,(W-H1-H2),THEN
            THICKNESSOFLAYER=(B*LAY*(RLOOP-1))/(W-H1-H2)
            R,RLOOP,THICKNESSOFLAYER        !THICKNESS

        *ELSE
        R,RLOOP,B                           !THICKNESS
        *ENDIF
        *ENDDO
*ENDIF



!DEFINITION ET, MAT, REAL STEEL********
ET,222,PLANE82,,,3
MP,EX,222,210E9
MP,PRXY,222,0.3
R,222,B
```

```
!ENTER OF KP********
K,1,0,0                    !CRACK TIP
K,2,H1
K,3,-(W-H1)
K,4,,(BN/2)
K,5,H1,(BN/2)
K,6,H1,(L/2)
K,7,-(W-H1),(L/2)
K,8,-(W-H1),(BN/2)
K,9,-(W-H1+HP),(0.2+(BP/2))
K,10,-(W-H1+HP),0.2
K,1001,-(W-H1),(0.2+(BP/2))
K,1002,-(W-H1),0.2

*DO,KCR,1,N-1,1     !STRING FOR THE CREATION OF THE NODES
   K,,-KCR*LAY
   K,,-KCR*LAY,(BN/2)
*ENDDO


!AREAS********
L,5,6        !L1
L,6,7        !L2
L,7,1001        !L3

A,1002,1001,9,10    !A1 STEEL
```

```
A,1,2,5,4                          !A2

A,1,4,12,11        !A3


*DO,ACR,1,N-2,1       !AREAS FROM 4 TO 4+(N-3)

   A,11+(ACR-1)*2,10+(ACR)*2,14+(ACR-1)*2,13+(ACR-1)*2

*ENDDO


A,(10+(N-1)*2)-1,10+(N-1)*2,8,3                    !AREA 4+(N-2)


L,8,1002         !L


FLST,2,(7+N-1),4

FITEM,2,1

FITEM,2,2

FITEM,2,3

FITEM,2,4

FITEM,2,(12+N*3)

FITEM,2,10

FITEM,2,12

*DO,ACR2,1,N-1,1

FITEM,2,(12+3*ACR2)

*ENDDO


AL,P51X
```

```
ALLSEL



!SIZE OF AREAS********

AESIZE,ALL,0.002,


!CREATION OF KSCON********

KSCON,4,ELSICRACK,1,ROZETA,0.75


!MESH CONCRETE

TYPE,1

MAT,1


*DO,AMESHLOOP,2,N+1,1    !MESHING OF AREAS

   REAL,AMESHLOOP

   AMESH,AMESHLOOP+1

*ENDDO


!MESH STEEL

AESIZE,ALL,0.002,

TYPE,222

MAT,222

REAL,222

AMESH,1


!MESH CONCRETE (ZERO THICKNESS)
```

```
TYPE,1

MAT,333

REAL,1

AMESH,2


AESIZE,ALL,0.01,   !MESHING OF THE BIGGEST AREA

R,(N+3),B              ! THE BIGGEST AREA

MAT,1

REAL,(N+3)

AMESH,(N+3)



!BOUNDARY CONDITIONS********

ALLSEL

LSEL,S,LOC,Y,0

LSEL,U,LINE,,7,8

NSLL,S,1

D,ALL,UY

ALLSEL


NSEL,S,LOC,X,H1

NSEL,R,LOC,Y,(S/2)-0.003,(S/2)+0.003

D,ALL,UX

ALLSEL


KSEL,S,KP,,10,10
```

```
NSLK

F,ALL,FX,FORCE

ALLSEL


EPLO

/SHRINK,0

/ESHAPE,1

/EFACET,1

/RATIO,1,1,1

/CFORMAT,32,0

/REPLOT




!CALCULATION**************************

/SOLU

SOLVE




!RESULTS**********************

/POST1

SET,FIRST


KSEL,S,KP,,4,4

NSLK
```

```
*GET, NCRACKTIP, NODE, 0, NUM, MIN
ALLSEL

NSEL,S,LOC,Y,(BN/2)          !NODE PRO POSUN V OSE LOZISKA
NSEL,R,LOC,X,ELSICRACK,0
NSEL,U,NODE,,NCRACKTIP

*GET, NUMBEROFNODES, NODE, 0, COUNT

    *IF,NUMBEROFNODES,EQ,2,THEN
    *GET, NMINKCALC, NODE, 0, NUM, MIN
    *GET, NMAXKCALC, NODE, 0, NUM, MAX
    NSEL,A,NODE,,NCRACKTIP
    LPATH,NCRACKTIP,NMAXKCALC,NMINKCALC  !NODES SELECTED
    KCALC,1,1,0,1

    *GET,KI1,KCALC,0,K,1              !MUST BE CHECKED

    !H2START2=(1-H2START)

    *VWRITE,N,ALPHA,H1,H2START,KI1
(F5.0,'  ',F5.3,'  ',F5.3,'  ',F5.3,'  ',F20.10)
!(F5.3,'              ',F20.10)
ALLSEL

    *ENDIF
```

```
/PREP7

ALLSEL

ACLEAR,ALL

ADEL,ALL

LDEL,ALL

KDEL,ALL


*ENDDO        !END H2 LOOP




!FINISH

!/CLEAR,NOSTART


*CFCLOSE                    !CLOSES TEXT DOCUMENT
```